DISS. ETH NO. 29371

Metabolic Insights from Coarse-Grained Modeling of multiple nutrient sources

A thesis submitted to attain the degree of

DOCTOR OF SCIENCES

(Dr. sc. ETH Zurich)

presented by

Ohad Golan

Master of Sciences, Tel-Aviv University, Israel
born on March 17th,1989
Citizen of Israel

accepted on the recommendation of
Prof. Dr. U. Sauer, examiner
Prof. Dr. S. Bonhoeffer, co-examiner
Prof. Dr. M. Basan, co-examiner

2023

מוקדש לסבי וסבותי,

על ערכים, בינה ואהבה

שהנחלתם בי

Contents

Abstract

Metabolism, the sum of biochemical processes that sustain life in an organism, is a complex network of intertwined reactions. These reactions facilitate the transformation of nutrients into energy and building blocks necessary for growth, reproduction, and maintaining cellular structures. Deciphering this intricate system is not only crucial for comprehending fundamental biological processes but is also central to numerous applications in biotechnology, health, and disease research.

Understanding and predicting the complexity of metabolic systems presents a formidable challenge. Each metabolic system constitutes an intricate web of concurrent reactions, intricately interlinked via sophisticated regulatory networks and feedback mechanisms. Additionally, these systems exhibit spatial and temporal dynamism, profoundly influenced by external determinants such as nutrient availability and environmental variables. Given the scale and complexity inherent in these systems, strictly experimental approaches often struggle to provide comprehensive insights. As such, a more holistic and integrative strategy is imperative for a thorough understanding of the nuanced intricacies of metabolic processes.

In light of this complexity, mathematical and computational modeling assert themselves as indispensable tools. They offer a systematic and quantitative approach to understand, analyze, and predict metabolic behavior. Mathematical models can integrate a myriad of biological details into a structured and manageable framework, enabling us to make sense of the data that experimental observations provide. By transposing our theoretical understanding of metabolic processes into a mathematical language, these models serve as a potent conduit, bridging the divide between empirical measurements and a holistic understanding of the system's behavior.

In this thesis, we utilize coarse-grained models to study fundamental questions concerning the physiology of autocatalytic systems. As a specialized class within the mathematical and computational modeling approaches, coarse-grained models serve as effective tools for

simplifying complex systems. By abstracting and reducing the level of detail, these models retain crucial components that accurately capture the system's overall behavior. They enable the distillation of numerous intricate reactions into key metabolic pathways or groups of reactions, rendering the inherent complexity of metabolic systems more tractable and interpretable. Using these models, we probe into the significant aspects of nutrient utilization and biomass generation in various growth conditions.

In **Chapter 1** we refined a quantitative framework, utilizing a coarse-grained proteome allocation model to study nutrient utilization in bacterial growth. Our focus is on the maintenance and yield coefficients in balanced growth conditions. We were able to elucidate the impact of distinct metabolic pathways, energy expenditure, and proteome allocation on these coefficients. Moreover, the model illuminates how various growth-limiting constraints affect cellular resource allocation under differing conditions. Notably, our analysis reveals that the maintenance coefficient, typically known to be influenced by the energy expenditures for maintenance processes and the efficiencies of active energy-generating pathways, is also affected by the size of non-active proteome sectors. Further extending the utility of this model, we present an approach to evaluate the cost of precursor biosynthesis including both the energetic and proteome costs.

In **Chapter 2**, we focus on nutrient utilization efficiency within a closed system, where all available nutrients are entirely consumed. We examine the implications of this scenario on biomass generation, particularly when growth involves multiple nutrients. To explore this, we built upon existing nutrient utilization models, commonly referred to as black box models, and extended them to incorporate the effects of multiple nutrients. Our research demonstrates that overall biomass yield is not solely reliant on nutrient availability, but also strongly influenced by the initial proportions of these nutrients. An intriguing observation was that supplementing specific nutrients could potentially trigger a decrease in biomass gain from others, adding another layer of complexity to the dynamics of nutrient utilization. Moreover, our methodology predicts the impact of each nutrient combination on broad metabolic processes, namely

catabolism, anabolism, or biomass precursor synthesis, offering intriguing insights for future investigations.

In the **Conclusions and outlook** section we encapsulate the significant contributions of this thesis towards enhancing our comprehension of nutrient utilization in bacterial growth and biomass generation. We evaluate the coarse-grained proteome allocation and black box models used in our research, offering critical insights into the role of model assumptions in metabolic modeling. We also envision the expansion of this work, suggesting the interconnection of the models to further decipher the mutual influence of multiple nutrient metabolism. The potential applications in the healthcare sector are also discussed, offering directions for future exploration. Furthermore, we critically analyze the current state of metabolic modeling, elucidating potential areas for development. From this vantage point, we propose a future path for metabolic modeling that lays greater emphasis on the underlying assumptions of the model, rather than primarily focusing on its mathematical formulation.

Zusammenfassung

Der Metabolismus ist die Summe der biochemischen Prozesse, die das Leben eines Organismus aufrechterhalten, und besteht aus einem komplexen Netzwerk von miteinander verflochtenen Reaktionen. Diese Reaktionen ermöglichen die Umwandlung von Nährstoffen in Energie und Bausteine, welche für Wachstum, Fortpflanzung und den Erhalt von Zellstrukturen notwendig sind. Dieses komplexe System besser zu verstehen ist nicht nur entscheidend für das Verständnis grundlegender biologischer Prozesse, sondern auch zentral für zahlreiche Anwendungen in Biotechnologie, Gesundheit und Krankheitsforschung.

Das Verständnis und die Vorhersage der Komplexität von Stoffwechselsystemen stellen eine große Herausforderung dar. Jedes Stoffwechselsystem besteht aus einem komplexen Netzwerk von gleichzeitig ablaufenden Reaktionen, die über ausgefeilte regulatorische Netzwerke und Feedbackmechanismen miteinander verknüpft sind. Darüber hinaus zeigen diese Systeme eine räumliche und zeitliche Dynamik, die stark von externen Faktoren wie der Verfügbarkeit von Nährstoffen und Umgebungsvariablen beeinflusst wird. Angesichts der Größe und Komplexität dieser Systeme stoßen rein experimentelle Ansätze oft an ihre Grenzen. Daher sind umfassendere und integrativere Strategien notwendig, um die Feinheiten von meatbolischen Prozesse zu verstehen.

Angesichts dieser Komplexität erweisen sich mathematische und rechnergestützte Modelle als unverzichtbare Werkzeuge. Sie bieten einen systematischen und quantitativen Ansatz zum Verständnis, zur Analyse und zur Vorhersage des metabolischen Verhaltens. Mathematische Modelle können eine Vielzahl von biologischen Details in einen strukturierten und handhabbaren Rahmen integrieren, der es uns ermöglicht, die Daten, die experimentelle Beobachtungen liefern, zu interpretieren. Indem sie unser theoretisches Verständnis von Stoffwechselprozessen in eine mathematische Sprache übersetzen, dienen diese Modelle als leistungsstarkes Bindeglied, das die Kluft zwischen empirischen Messungen und einem ganzheitlichen Verständnis des Systemverhaltens überbrückt.

In dieser Dissertation nutzen wir grobkörnige (vereinfachte) Modelle, um grundlegende Fragen zur Physiologie von autokatalytischen Systemen zu untersuchen. Als spezialisierte Klasse innerhalb der mathematischen und rechnergestützten Modellierungsansätze dienen grobkörnige Modelle als wirksame Werkzeuge zur Vereinfachung komplexer Systeme. Durch die Abstraktion und Reduzierung des Detailgrades behalten diese Modelle wesentliche Komponenten bei, die das Gesamtverhalten des Systems erfassen. Sie ermöglichen es, zahlreiche komplexe Reaktionen auf Schlüsselstoffwechselwege oder Gruppen von Reaktionen zu begrenzen, was die inhärente Komplexität von Stoffwechselsystemen handhabbarer und interpretierbarer macht. Mit diesen Modellen gehen wir wichtigen Aspekten der Nährstoffnutzung und Biomasseerzeugung in verschiedenen Wachstumsbedingungen auf den Grund.

Im **Kapitel 1** haben wir einen quantitativen Rahmen weiterentwickelt und ein grobkörniges Proteomallokationsmodell zur Untersuchung der Nährstoffnutzung im bakteriellen Wachstum verwendet. Unser Fokus liegt auf den Instandhaltungs- und Ertragskoeffizienten in ausgewogenen Wachstumsbedingungen. Wir konnten die Auswirkungen von unterschiedlichen Stoffwechselwegen, Energieaufwendungen und Proteomzuteilungen auf diese Koeffizienten aufzeigen. Darüber hinaus beleuchtet das Modell, wie verschiedene wachstumsbegrenzende Faktoren die zelluläre Ressourcenallokation unter unterschiedlichen Bedingungen beeinflussen. Bemerkenswert ist, dass unsere Analyse zeigt, dass der Instandhaltungskoeffizient, der in der Regel durch die Energieaufwendungen für Instandhaltungsprozesse und die Effizienz aktiver Energieerzeugungswege beeinflusst wird, auch durch die Größe der nicht aktiven Proteomsektoren beeinflusst wird. Darüber hinaus präsentieren wir einen Ansatz zur Bewertung der Kosten der Vorläuferbiosynthese, einschließlich der energetischen und Proteomkosten.

In **Kapitel 2** konzentrieren wir uns auf die Nährstoffverwertungseffizienz in einem geschlossenen System, in dem alle verfügbaren Nährstoffe vollständig verbraucht werden. Wir untersuchen die Auswirkungen dieses Szenarios auf die Biomassebildung, insbesondere

wenn das Wachstum mehrere Nährstoffe beinhaltet. Um dies zu untersuchen, haben wir auf bestehende Nährstoffnutzungsmodelle, die üblicherweise als "Black-Box"-Modelle bezeichnet werden, aufgebaut und sie erweitert, um die Auswirkungen von mehreren Nährstoffen zu berücksichtigen. Unsere Forschung zeigt, dass der gesamte Biomasseertrag nicht nur von der Verfügbarkeit der Nährstoffe abhängt, sondern auch stark von den ursprünglichen Anteilen dieser Nährstoffe beeinflusst wird. Eine interessante Beobachtung war, dass die Ergänzung bestimmter Nährstoffe potenziell einen Rückgang der Biomassezunahme aus anderen auslösen könnte, was eine weitere Ebene der Komplexität zu der Dynamik der Nährstoffnutzung hinzufügt. Darüber hinaus prognostiziert unsere Methode den Einfluss jeder Nährstoffkombination auf breite Stoffwechselprozesse, nämlich Katabolismus, Anabolismus oder Biomasse-Vorläufersynthese, und bietet faszinierende Einblicke für zukünftige Untersuchungen.

Im **Abschnitt Schlussfolgerungen und Ausblick** fassen wir die wesentlichen Beiträge dieser Dissertation zur Verbesserung unseres Verständnisses der Nährstoffnutzung im bakteriellen Wachstum und der Biomasseerzeugung zusammen. Wir bewerten die grobkörnigen Proteomallokations- und Black-Box-Modelle, die in unserer Forschung verwendet wurden, und bieten kritische Einblicke in die Rolle von Modellannahmen in der metabolischen Modellierung. Wir skizzieren auch die Erweiterung dieser Arbeit und schlagen die Verbindung der Modelle vor, um den gegenseitigen Einfluss des mehrfachen Nährstoffmetabolismus weiter zu entschlüsseln. Die potenziellen Anwendungen im Gesundheitssektor werden ebenfalls diskutiert und bieten Richtungen für zukünftige Erkundungen. Darüber hinaus analysieren wir den aktuellen Stand der metabolischen Modellierung kritisch und beleuchten potenzielle Entwicklungsbereiche. Von diesem Standpunkt aus schlagen wir einen zukünftigen Weg für die metabolische Modellierung vor, der mehr Gewicht auf die zugrundeliegenden Annahmen des Modells legt, anstatt sich hauptsächlich auf seine mathematische Formulierung zu konzentrieren.

Chapter 1 – General introduction

Ohad Golan[1, 2]

[1] Institute of Molecular Systems Biology, ETH Zürich, Otto-Stern-Weg 3, 8093 Zürich, Switzerland

[2] Life Science Zurich PhD Program on Systems Biology, Zurich, Switzerland

Ohad Golan wrote the chapter.

Andrea Weisse, Hidde de Jong read for correction sections: ‘Bacterial growth laws’ and ‘Mathematical models of microbial growth’.

Uwe Sauer read for correction.

Bacterial growth

A fundamental characteristic of living systems is their capacity for growth and reproduction [1,2]. The reproductive success of a living system in a given environment determines its fitness. The study of the growth of bacteria and other microorganisms is crucial for better understanding their capacity to cause diseases in humans or for better exploiting their use in biotechnological or environmental processes. Beyond their numerous practical applications, bacteria and other microorganisms have emerged as ideal model systems for investigating fundamental questions surrounding the relationship between growth, fitness, and environmental characteristics.

Microbial growth entails the uptake of nutrients from the environment and their conversion into new microbial cells through a series of interconnected metabolic processes. This highlights the self-replicating or autocatalytic nature of microbial growth [3–8], wherein cells transform environmental nutrients into new cells (fig. 1A). In this thesis, we consider growth on the population level, that is, an increase in the total amount of cells or, equivalently in many situations, an increase of the overall biomass of the population. This perspective leads to the well-known model of microbial growth, where the growth in biomass over time is proportional to the existing biomass resulting in exponential growth [2].

Classical experiments for microbial growth are known as batch culture experiments, in which bacteria are inoculated into a medium containing limited resources [1]. The growth of the bacterial population as a function of time is monitored, revealing a characteristic bacterial growth curve which is generally separated into three distinct phases [9–11] (fig. 1B): the lag phase, the exponential growth phase, and the stationary phase, each characterized by specific growth dynamics and physiology. Initially, the bacteria take time to adapt to the new conditions before they start growing, this is the lag phase. Following this adjustment, the bacteria enter the exponential growth phase, where they proliferate rapidly. When a limiting nutrient is depleted, the bacteria cease to grow, entering the stationary phase.

Bacterial growth laws

One of the first to study the growth of bacterial cultures systematically and quantitatively was Jacques Monod in the 1940s [12]. He characterized bacterial growth by means of batch culture experiments in a well-defined growth medium studying the different phases of the bacterial growth curve. Together with the chemostat, a device allowing continuous culture of microorganisms at a predefined growth rate [13–16], these methods have become standard in microbial physiology. They notably underlie the discovery of a number of so-called growth laws, relating the growth rate to a variety of properties of the physiology of growing bacteria [17–19]. The growth laws are conserved across different organisms and a broad range of experimental conditions. Here, we list three examples of well-known growth laws:

1. **Dependency of the growth rate on nutrient availability** [1,9,11]**:** In his characterization of bacterial growth, Monod discovered the first growth law. He observed that the growth rate of bacteria depends upon the nutrient concentration in the medium in a hyperbolic fashion (fig. 2A).
2. **Correlation between growth rate and nutrient uptake rate** [14–16,20,21]**:** In continuous cultures, the growth rate was shown to vary linearly with the nutrient uptake rate (fig. 2B). The slope of this linear relation is called the biomass yield and the offset the ‘maintenance energy’, as it is assumed to be derived from the energy spent on processes required to maintain the basic processes of the cell, in the absence of growth [20,22–24].
3. **Correlation between growth rate and cellular composition** [25,26]**:** In 1959, Schaechter, Maaløe and Kjeldgaard showed that RNA, DNA and the number of nuclei in *Salmonella typhimurium* linearly correlate with the growth rate [25]. Later, it was further shown that other physiological parameters, such as the mass fraction of ribosomes in growing populations, also linearly correlate with the growth rate (fig. 2C) [26]. Initially, it was believed that the correlation between ribosomal mass fraction and growth was strictly positive, however, Scott et al. [27] showed that when growth is

inhibited through translation-inhibiting drugs, growth rate and ribosomal mass fraction exhibit a negative (near-)linear relation.

Mathematical models of microbial growth

The conserved nature of the growth laws has led scientists to ask whether there are fundamental principles governing bacterial growth. To answer this question, different types of mathematical models have been developed. One approach aims at integrating all known molecular constituents of the cell and the reactions involving these constituents into a big model, an in-silico copy, or 'digital twin', of the cell. Such models, known as fine-grained models, can be useful to predict emergent phenotypes [28–31], but they are difficult to construct and maintain, and their complexity makes it hard to grasp certain principles that underpin growth. In this thesis, we will focus on coarse-grained models of bacterial growth. Rather than assembling individual reactions in a bottom-up manner, these models are based on the top-down definition of a limited number of basic cellular functions or processes involved in growth, described by appropriate macro-reactions [32,33] (fig. 3). Coarse-grained models are smaller and therefore easier to construct and analyze. The lack of molecular detail can make their predictions less accurate, but their simplicity allows a focus on how basic cellular functions and their interactions shape bacterial growth. How much detail is included in a model, also known as its granularity, and which assumptions are considered depends on the specific scientific question asked.

Fundamental assumptions in mathematical models of microbial growth

All mathematical models of microbial growth, irrespective of their granularity, are based on a set of fundamental assumptions that follow from biochemical and biophysical constraints. These assumptions serve as the foundations upon which the structure and equations of the model are built. Each model utilizes the assumptions relevant to the scientific question it seeks to address, allowing it to abstract and simplify the complex reality of microbial growth while

retaining the essential aspects necessary for the investigation. In this section, we enumerate the most prominent assumptions that underpin various models of microbial growth.

Conservation of mass and quasi-steady-state assumption

According to the law of mass conservation, the change of mass is equal to the inflow minus the outflow of mass. Therefore, the change in concentration of a cell component, for example a metabolite, is determined by the sum of the rates of the reactions consuming and producing this cell component (fig. 4A). When the incoming and outgoing flux of a cell component are equal, the concentration of the cell component is constant in time. A quasi-steady-state assumption states that the concentration of all cell components is constant in time. This is a typical assumption that simplifies the mathematical analysis of the system significantly and holds for growth in constant conditions known as balanced growth.

Proteome allocation assumption

The biochemical reactions breaking down nutrients into intracellular metabolites, and the reactions utilizing these metabolites for the synthesis of new biomass, do not occur spontaneously. The reactions are catalyzed mostly by proteins complexes, in particular metabolic enzymes and ribosomes.

In fine-grained models, the components of each biochemical reaction including the proteins catalyze it and each substrate are described separately. Alternatively, in coarse-grained models, well-defined sets of biochemical reactions are grouped together into macro-reactions. The cell components that are necessary to catalyze the individual steps of a macro-reaction are grouped together into a corresponding so-called proteome sector. A proteome sector includes mostly proteins that catalyze metabolic reactions but also ribosomes catalyzing the reaction of protein biosynthesis.

Proteins constitute most of the biomass of the cell [34]. As a first approximation, therefore, the sum of the proteins or the proteome sectors equals the total biomass of the growing population. The proteins or proteome sectors mass as defined above are extensive quantities, summed

over the entire growing population. For the models, we are rather interested in intensive quantities, the amount of a proteome sector relative to the total amount of biomass (protein), corresponding to protein concentrations or protein fractions. As such, it is convenient to divide the protein mass, or proteome sector mass by the total cell mass and work with dimensionless or protein or proteome fractions that sum up to one [35,36] (fig. 4B).

Mathematical description of reaction fluxes

The rate at which a reaction is converting one cell component, e.g., a metabolite, into another is determined by the amount of enzymes carrying out this reaction (fine-grained model) or size of the relevant proteome fraction (coarse-grained model), the efficiency of the enzymes or proteome sector, the concentrations of the substrates of the reaction and possible regulation by other cell components in the system. While mass-action kinetics provide a principled framework to develop rate equations for biochemical reactions, in practice, various approximations based on mechanistic assumptions are often used to obtain simplified equations. The simplest relation of the flux to the relevant proteome sector is linear. This expression assumes that the substrates are in excess and disregards any regulation of the flux by allosteric interactions of the enzymes and other cell components. While this assumption simplifies the model, it is lacking in the realistic details. A more complex relation is obtained when the substrate is not in excess and allosteric interactions involving other cell components play a role in the modulation of the flux [37–41]. The expression of the flux is multiplied by regulatory functions describing the modulation of the flux by the substrate and the allosteric cell component. Typically, a Michaelis-Menten relation is taken for the effect of the concentration of substrate on the flux (fig. 4C).

Volume and surface area assumptions

The intracellular volume as well as the surface area of the cell are limited. Obviously, the total volume occupied by the components of the cell, in particular proteins, cannot be larger than the cell volume. As such, the total volume of the cell is larger than the sum of the volume of the proteome sectors that are functioning inside [42,43] (fig. 4D). Other cell components such

as the DNA strands can be considered by adding a factor to the volume of the cell components. Similarly, the total surface occupied by proteins and lipids making up the cell membrane must equal the surface area of the cell [44].

Further assumptions in modeling of microbial growth

Due to the complexity of the biological systems, additional assumptions that are not strictly based on biophysical and biochemical constraints are often necessary to model metabolism effectively. These include phenomenological assumptions, which are based on prior experimental data [45–48] without understanding the forces involved and usually establish a relationship between physiological parameters and internal constituents. For instance, empirical observations showing a linear relationship between the growth rate and the number of ribosomes [26] (fig. 2C) lead to a mathematical constraint in the model, stipulating that the portion of the proteome that includes the ribosomes is always linearly related to the growth rate.

Another set of assumptions is based on the optimization principle. This principle stems from the understanding that biological systems, having evolved over millions of years, operate in a way that optimizes certain objectives [49]. This optimization is not arbitrary but is rather a reflection of the selective pressures exerted on these systems over evolutionary time. As an illustration, microbes in natural environments are persistently engaged in resource competition, not only with members of their own species but also with other organisms. One strategy to compete for resources and ensure survival is to grow faster than competitors [50,51], thereby securing access to resources earlier. Consequently, in environments characterized by such competition, the fastest growing microbes are likely to survive and be evolutionarily selected. This survival of the fittest lends credibility to the assumption that metabolism is shaped by evolution to optimize the growth rate, an assumption that features prominently in many metabolic models. [52–55].

While the principle of growth rate maximization is frequently employed in metabolic modeling, it may not always be applicable or optimal [56]. Growth depends on a variety of factors, such

as nutrient availability, temperature, and acidity, to name a few. While a microbe might optimize its metabolic pathways for rapid growth in nutrient-rich, stress-free environments, such ideal conditions may not be sustainable over time. Organisms can encounter sudden environmental shifts, including nutrient scarcity or the presence of toxins, necessitating a recalibration of their survival strategy. In such stressful circumstances, a singular focus on maximizing growth rate might not be the most advantageous approach [57]. Rather, microbes that have allocated resources towards stress resistance mechanisms may demonstrate enhanced adaptability and survival potential [58]. This scenario exemplifies a crucial trade-off that organisms face: the optimization of growth rates versus the investment in stress resistance mechanisms. These trade-offs are integral to the nuance of microbial metabolic modeling, as models aim to encapsulate cellular strategies in diverse environments and elucidate the complex trade-offs faced by cells [59,60].

Model examples

Several modeling methods have emerged as pillars in the field of metabolic modeling, each with its unique strengths and applications. These models employ different levels of granularity and utilize a variety of mathematical frameworks and assumptions. Here, we will present some of the most prominent modeling methods.

Flux balance analysis

Flux Balance Analysis (FBA) is a cornerstone of genome-scale metabolic models for exploring biochemical networks. It has found widespread use in systems biology and metabolic engineering, enabling the calculation of the flow or "flux" of metabolites through a metabolic network, hence the terminology "Flux Balance Analysis." FBA is built upon assumptions of mass conservation and steady state, along with phenomenological assumptions to set bounds on flux rates. The methodology translates the system of biochemical reactions into a set of linear equations and assumes the system optimizes an objective function, typically the growth rate [61–63].

Since its inception in the 1990s, FBA has continually evolved to incorporate additional constraints and assumptions. These advancements include considerations of proteome allocation [64–67], gene regulation [68–70] and the impact of thermodynamic effects on reaction fluxes [71,72]. FBA has been extended to generate dynamic profiles of cell growth as well as substrate and by-product concentrations [73–76]. While FBA has proven to be a powerful tool for understanding and engineering metabolism, it is essential to recognize that its base assumptions may not always be valid and its high level of detail make it difficult to deduct general conclusions. Furthermore, it necessitates a comprehensive and accurate metabolic network reconstruction, which may not always be accessible.

Metabolism and expression models

Metabolism and Expression (ME) models represent an advanced genre of genome-scale metabolic models, encompassing both metabolic processes and protein expression mechanisms [77]. Unlike FBA models, ME models incorporate information about the gene expression machinery necessary for the production of the enzymes catalyzing metabolic reactions. This integrated perspective allows for a more comprehensive understanding of a cell's metabolic capabilities, factoring in the proteome and mass balance assumptions as well as the costs of gene expression machinery. ME models offer the ability to predict the impacts of various genetic and environmental perturbations on microbial growth [77]. They yield insights into how cells distribute their resources under diverse conditions and illuminate how alterations in gene expression can precipitate different metabolic phenotypes [78–80]. However, ME models, while powerful, are relatively complex, require significant computational resources to solve, and like FBA models necessitate detailed information about the organism's metabolic and protein expression systems, which may not always be available.

Coarse-grained proteome allocation models

Coarse-grained proteome allocation models serve as an efficient approach to simplifying the intricacies of biological systems, focusing on broader components or behaviors rather than capturing every minute detail. Formulated as resource allocation problems, these models

concentrate on the proteome constraint and how it is allocated across the cell pathways. Such models have proven instrumental in elucidating the fundamental trade-offs that cells navigate when faced with competing demands, such as balancing growth and stress response [81,82] or optimizing the use of alternative metabolic pathways [52,83]. Furthermore, these models shed light on the regulatory mechanisms of metabolic pathways such as allosteric regulation [56,84]. Despite relying on simplifying assumptions and potentially omitting certain complexities of the biological system, they provide valuable insights into the fundamental principles governing proteome allocation and predict cellular responses to different conditions or perturbations.

Mechanistic models

Mechanistic models simulate growth based on a thorough understanding of the integral biological processes involved. These models aim to consolidate our existing knowledge of all mechanisms within the system, thereby deriving holistic inferences about the system's comprehensive behavior. Typically not relying on phenomenological or optimization assumptions, they prioritize inherent biochemical and biophysical interactions that underpin system dynamics. They encompass a wide range of scales, extending from molecular and cellular models to those pertaining to tissues, organs, and entire organisms, highlighting their utility in capturing complex biological phenomena at varying levels of detail [60,85,86].

Self-replicating systems beyond biology

Thus far, we have elucidated the principles of microbial metabolism and the mathematical models employed to enhance our understanding of it. In this section, we aim to extend the purview of metabolism beyond biological systems, thereby broadening the applicability of these models to other domains. The term "metabolism" typically describes the collection of chemical reactions within biological organisms that synthesize and transform molecules essential for life. While this definition is useful, it gives no scientific or mathematical ground for the analysis of metabolic systems. To address this, we propose a broader interpretation of metabolic systems and begin with a more formal definition that can be applied beyond the

confines of biological systems. We us a definition of a metabolic system as a "well-defined system that absorbs nutrients and utilizes them to sustain itself" [87–89].

To illustrate the breadth of our definition of a metabolic system, let's consider an example outside the sphere of biology: an economic entity, specifically, a construction firm. Analogous to a cell's intake of nutrients, the construction firm sources raw materials like steel, cement, and wood, along with skilled labor and financial resources. These inputs, similar to a cell's nutrients, are integral to the firm's survival and growth. The firm's workforce, akin to the enzymes within a cell, then facilitates the transformation of these raw materials into a finished product – the building. This process mirrors a cell's conversion of nutrients into biomolecules necessary for its survival and proliferation.

In essence, just as a biological cell represents a metabolic system that absorbs nutrients and utilizes them for self-sustenance, a construction firm can similarly be perceived as a metabolic system within the economic domain, ingesting raw materials and resources to maintain its operations and promote growth [87]. Expanding upon this analogy, it is important to note that, since a construction firm aligns within our definition of a metabolic system, the mathematical models described in this work can also be applied to this context. These models can provide insights into the resource allocation and efficiency of the firm's operations, just as they do for biological systems. This highlights the universality and versatility of our mathematical framework, demonstrating its potential utility beyond the realm of biological metabolism.

Thesis outline

In this **Introduction**, we delineate the fundamentals of bacterial growth, outline the primary assumptions employed in the modeling of bacterial growth, and provide illustrative examples of such models. In **Chapter 1** we present a refined coarse-grained proteome allocation model, elucidating the complex interplay between cellular processes and physiological growth parameters. In **Chapter 2** we explore the reciprocal effects of varying nutrient combinations on microbial biomass yield, employing a coarse-grained thermodynamic model to encapsulate these effects. Finally, in the **Conclusions and outlook** section, we outline the major

conclusions of this thesis, discuss the future trajectory of metabolic models and their applications.

Figures

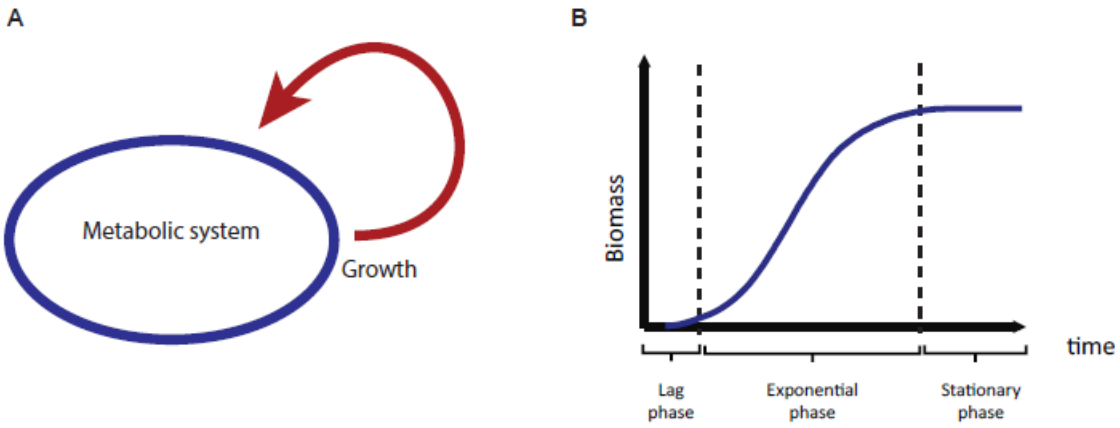

Figure 1 – Microbial growth. (A) An autocatalytic system. **(B)** A microbial growth curve. Inoculation of microbes in an environment with limited nutrients begins with a lag time until the microbes adjust to the new environment. It is followed by the exponential growth phase in which the microbes reproduce rapidly. When the nutrients in the environment are depleted, the microbes stop reproducing and stationary phase is reached.

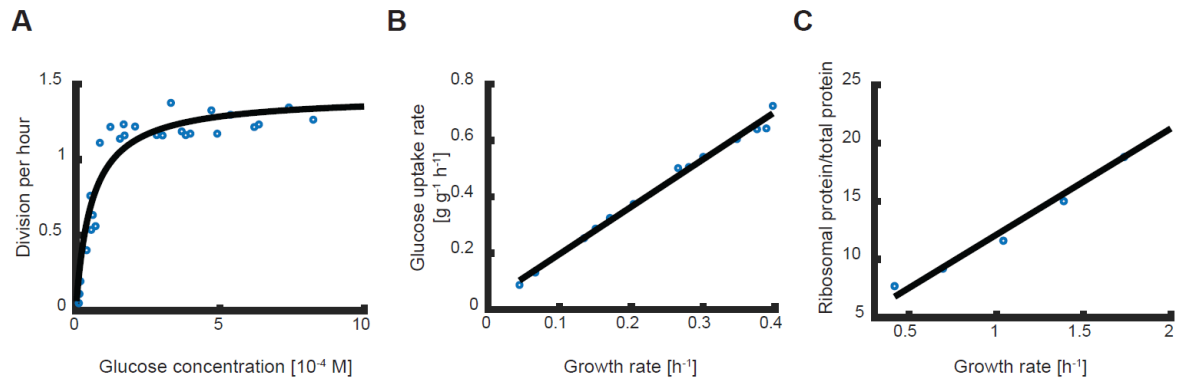

Figure 2 – Microbial growth laws. (A) Monod growth law: growth rate dependency on nutrient availability. In this example, the nutrient is the sugar glucose [Data from [1]] **(B)** Correlation between growth rate and nutrient uptake rate. In this example, the nutrient is the sugar glucose [Data from [90]]. **(C)** Correlation between growth rate and cellular composition. In this example of the concentration of ribosomes [Data from [26]].

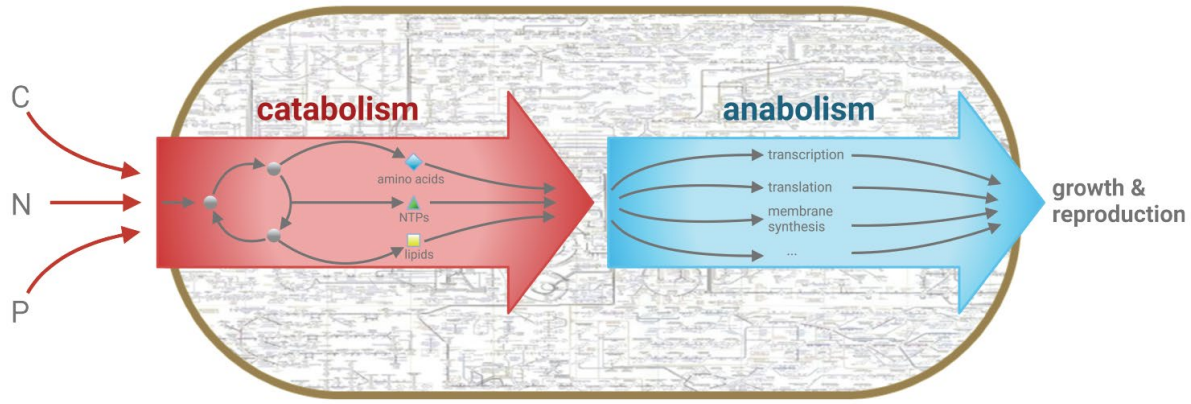

Figure 3 – Coarse grained modeling of metabolism. Compared to genome-scale and whole-cell models, coarse grained models zoom out of the molecular detail and focus on key processes.

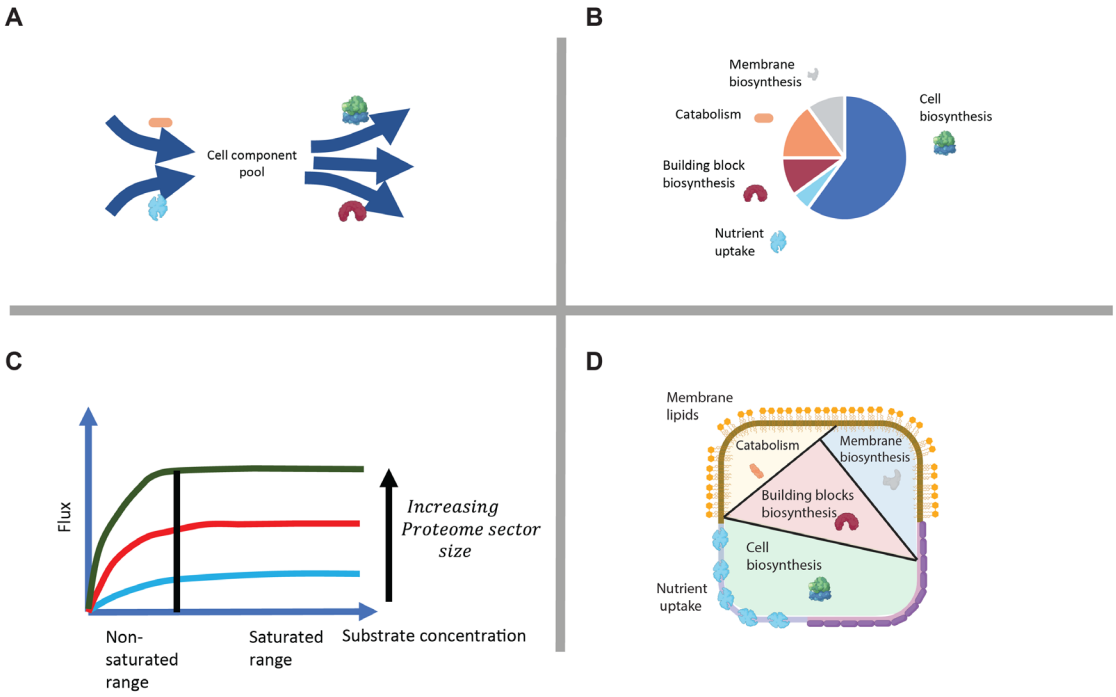

Figure 4 – Fundamental assumptions in the modeling of microbial growth. (A) Conservation of mass and steady-state assumption: The change in concentration of a cell component is equal to the incoming flux minus the outgoing flux. At steady state, the concentration of the cell component is constant. **(B)** Proteome allocation assumption: the proteome is divided into different proteome sectors. The number of proteome sectors in a model depends on the model granularity. The sum of all the proteome sectors always equals 1. **(C)** Example of flux assumption according to Michaelis-Menten kinetics: the reaction is carried out by proteome sector. The maximal rate is reached for saturating substrate concentrations and is determined by the size of the proteome sector. **(D)** Volume and surface area assumption: schematic representation showing the volume of the cell is limited and is filled with intracellular cell components such as proteins. The sum of the volumes of the intracellular cell components is equal to the cell volume. Similarly, the surface area of the cell is limited and contains membrane cell components such as lipids. The sum of the surface areas of membrane cell components is equal to the cell surface area.

References

1. Monod J. The growth of bacterial cultures. Annu Rev Microbiol. 1949;3: 371–394.
2. Neidhardt FC. Bacterial growth: constant obsession with dN/dt. J Bacteriol. 1999;181: 7405–7408.
3. Wang T, Sha R, Dreyfus R, Leunissen ME, Maass C, Pine DJ, et al. Self-replication of information-bearing nanoscale patterns. Nature. 2011;478: 225–228.
4. Schulman R, Yurke B, Winfree E. Robust self-replication of combinatorial information via crystal growth and scission. Proceedings of the national academy of sciences. 2012;109: 6405–6410.
5. Paul N, Joyce GF. Minimal self-replicating systems. Curr Opin Chem Biol. 2004;8: 634–639.
6. Griffith S, Goldwater D, Jacobson JM. Self-replication from random parts. Nature. 2005;437: 636.
7. Zykov V, Mytilinaios E, Adams B, Lipson H. Self-reproducing machines. Nature. 2005;435: 163–164.
8. Neumann J von. Theory of self-reproducing automata. Math Comput. 1966;21: 745.
9. Schaechter M. A brief history of bacterial growth physiology. Front Microbiol. 2015;6: 289.
10. Widdel F. Theory and measurement of bacterial growth. Di dalam Grundpraktikum Mikrobiologie. 2007;4: 1–11.
11. Paulton RJL. The bacterial growth curve. J Biol Educ. 1991;25: 92–94.
12. Monod J. Recherches sur la croissance des cultures bacteriennes. 1942.
13. Novick A, Szilard L. Description of the chemostat. Science. 1950;112: 715–716.
14. Ziv N, Brandt NJ, Gresham D. The use of chemostats in microbial systems biology. JoVE (Journal of Visualized Experiments). 2013; e50168.
15. Kuenen G. Continuous cultures (chemostats). Encyclopedia of microbiology. Elsevier; 2019. pp. 743–761.
16. Smith HL, Waltman P. The theory of the chemostat: dynamics of microbial competition. Cambridge university press; 1995.
17. Jun S, Si F, Pugatch R, Scott M. Fundamental principles in bacterial physiology—history, recent progress, and the future with focus on cell size control: a review. Reports on Progress in Physics. 2018;81: 056601.
18. Scott M, Hwa T. Bacterial growth laws and their applications. Curr Opin Biotechnol. 2011;22: 559–565.
19. Roy A, Goberman D, Pugatch R. A unifying autocatalytic network-based framework for bacterial growth laws. Proceedings of the National Academy of Sciences. 2021;118: e2107829118.

20. Pirt SJ. The maintenance energy of bacteria in growing cultures. Proc R Soc Lond B Biol Sci. 1965;163: 224–231.

21. Novick A, Szilard L. Description of the chemostat. Science. 1950;112: 715–716.

22. Van Bodegom M, Homberg JR, Henckens MJAG. Modulation of the hypothalamic-pituitary-adrenal axis by early life stress exposure. Front Cell Neurosci. 2017;11: 87.

23. Marr AG, Nilson EH, Clark DJ. The maintenance requirement of Escherichia coli. Ann N Y Acad Sci. 1963;102: 536–548.

24. Tempest DW, Neijssel OM. The status of YATP and maintenance energy as biologically interpretable phenomena. Annu Rev Microbiol. 1984;38: 459–513.

25. Schaechter M, Maaløe O, Kjeldgaard NO. Dependency on medium and temperature of cell size and chemical composition during balanced growth of Salmonella typhimurium. Microbiology (N Y). 1958;19: 592–606.

26. Bremer H, Dennis PP. Modulation of chemical composition and other parameters of the cell at different exponential growth rates. EcoSal Plus. 2008;3.

27. Scott M, Gunderson CW, Mateescu EM, Zhang Z, Hwa T. Interdependence of cell growth and gene expression: origins and consequences. Science. 2010;330: 1099–1102.

28. O'Brien EJ, Monk JM, Palsson BO. Using Genome-scale Models to Predict Biological Capabilities. Cell. 2015;161: 971–987. doi:https://doi.org/10.1016/j.cell.2015.05.019

29. Price ND, Reed JL, Palsson BØ. Genome-scale models of microbial cells: evaluating the consequences of constraints. Nat Rev Microbiol. 2004;2: 886–897.

30. Fang X, Lloyd CJ, Palsson BO. Reconstructing organisms in silico: genome-scale models and their emerging applications. Nat Rev Microbiol. 2020;18: 731–743.

31. Gu C, Kim GB, Kim WJ, Kim HU, Lee SY. Current status and applications of genome-scale metabolic models. Genome Biol. 2019;20: 121. doi:10.1186/s13059-019-1730-3

32. Scott M, Hwa T. Shaping bacterial gene expression by physiological and proteome allocation constraints. Nat Rev Microbiol. 2023;21: 327–342. doi:10.1038/s41579-022-00818-6

33. Doan DT, Hoang MD, Heins A-L, Kremling A. Applications of Coarse-Grained Models in Metabolic Engineering. Front Mol Biosci. 2022;9.

34. Neidhardt FC. Escherichia coli and Salmonella: cellular and molecular biology. 1996.

35. Chen Y, Nielsen J. Mathematical modeling of proteome constraints within metabolism. Curr Opin Syst Biol. 2021;25: 50–56.

36. O'Brien EJ, Palsson BO. Computing the functional proteome: recent progress and future prospects for genome-scale models. Curr Opin Biotechnol. 2015;34: 125–134.

37. Cleland W. Enzyme kinetics. Annu Rev Biochem. 1967;36: 77–112.

38. Cornish-Bowden A. The origins of enzyme kinetics. FEBS Lett. 2013;587: 2725–2730.

39. Vasic-Racki D, Kragl U, Liese A. Benefits of enzyme kinetics modelling. Chem Biochem Eng Q. 2003;17: 7–18.

40. Seibert E, Tracy TS. Fundamentals of enzyme kinetics. Enzyme Kinetics in Drug Metabolism: Fundamentals and Applications. 2014; 9–22.

41. van Eunen K, Bakker BM. The importance and challenges of in vivo-like enzyme kinetics. Perspect Sci (Neth). 2014;1: 126–130.

42. Dill KA, Ghosh K, Schmit JD. Physical limits of cells and proteomes. Proceedings of the National Academy of Sciences. 2011;108: 17876–17882.

43. Zadrag-Tecza R, Kwolek-Mirek M, Bartosz G, Bilinski T. Cell volume as a factor limiting the replicative lifespan of the yeast Saccharomyces cerevisiae. Biogerontology. 2009;10: 481–488.

44. Szenk M, Dill KA, de Graff AMR. Why Do Fast-Growing Bacteria Enter Overflow Metabolism? Testing the Membrane Real Estate Hypothesis. Cell Syst. 2017;5: 95–104. doi:10.1016/j.cels.2017.06.005

45. Esser DS, Leveau JHJ, Meyer KM. Modeling microbial growth and dynamics. Appl Microbiol Biotechnol. 2015;99: 8831–8846.

46. Dutta D, Saini S. Phenomenological models as effective tools to discover cellular design principles. Arch Microbiol. 2019;201: 283–293.

47. Peleg M, Corradini MG. Microbial growth curves: what the models tell us and what they cannot. Crit Rev Food Sci Nutr. 2011;51: 917–945.

48. Lema-Perez L, Muñoz-Tamayo R, Garcia-Tirado J, Alvarez H. On parameter interpretability of phenomenological-based semiphysical models in biology. Inform Med Unlocked. 2019;15: 100158.

49. Berkhout J, Bruggeman FJ, Teusink B. Optimality principles in the regulation of metabolic networks. Metabolites. 2012;2: 529–552.

50. Ghoul M, Mitri S. The ecology and evolution of microbial competition. Trends Microbiol. 2016;24: 833–845.

51. MacLean RC, Gudelj I. Resource competition and social conflict in experimental populations of yeast. Nature. 2006;441: 498–501.

52. Molenaar D, Van Berlo R, De Ridder D, Teusink B. Shifts in growth strategies reflect tradeoffs in cellular economics. Mol Syst Biol. 2009;5: 323.

53. O'brien EJ, Lerman JA, Chang RL, Hyduke DR, Palsson BØ. Genome-scale models of metabolism and gene expression extend and refine growth phenotype prediction. Mol Syst Biol. 2013;9: 693.

54. Ibarra RU, Edwards JS, Palsson BO. Escherichia coli K-12 undergoes adaptive evolution to achieve in silico predicted optimal growth. Nature. 2002;420: 186–189.

55. Bosdriesz E, Molenaar D, Teusink B, Bruggeman FJ. How fast-growing bacteria robustly tune their ribosome concentration to approximate growth-rate maximization. FEBS J. 2015;282: 2029–2044.

56. Towbin BD, Korem Y, Bren A, Doron S, Sorek R, Alon U. Optimality and sub-optimality in a bacterial growth law. Nat Commun. 2017;8: 14123.

57. Cheng C, O'brien EJ, McCloskey D, Utrilla J, Olson C, LaCroix RA, et al. Laboratory evolution reveals a two-dimensional rate-yield tradeoff in microbial metabolism. PLoS Comput Biol. 2019;15: e1007066.

58. Basan M, Honda T, Christodoulou D, Hörl M, Chang Y-F, Leoncini E, et al. A universal trade-off between growth and lag in fluctuating environments. Nature. 2020;584: 470–474.

59. Beardmore RE, Gudelj I, Lipson DA, Hurst LD. Metabolic trade-offs and the maintenance of the fittest and the flattest. Nature. 2011;472: 342–346. doi:10.1038/nature09905

60. Weiße AY, Oyarzún DA, Danos V, Swain PS. Mechanistic links between cellular trade-offs, gene expression, and growth. Proceedings of the National Academy of Sciences. 2015;112: E1038–E1047. doi:10.1073/pnas.1416533112

61. Gianchandani EP, Chavali AK, Papin JA. The application of flux balance analysis in systems biology. Wiley Interdiscip Rev Syst Biol Med. 2010;2: 372–382.

62. Raman K, Chandra N. Flux balance analysis of biological systems: applications and challenges. Brief Bioinform. 2009;10: 435–449. doi:10.1093/bib/bbp011

63. Orth JD, Thiele I, Palsson BØ. What is flux balance analysis? Nat Biotechnol. 2010;28: 245–248. doi:10.1038/nbt.1614

64. Zeng H, Yang A. Flux Balance Analysis Incorporating a Coarse-grained Proteome Constraint for Predicting Overflow Metabolism in Escherichia Coli. In: Kiss AA, Zondervan E, Lakerveld R, Özkan L, editors. Computer Aided Chemical Engineering. Elsevier; 2019. pp. 865–870. doi:https://doi.org/10.1016/B978-0-12-818634-3.50145-4

65. Zeng H, Yang A. Bridging substrate intake kinetics and bacterial growth phenotypes with flux balance analysis incorporating proteome allocation. Sci Rep. 2020;10: 4283.

66. Goelzer A, Fromion V, Scorletti G. Cell design in bacteria as a convex optimization problem. Automatica. 2011;47: 1210–1218.

67. Goelzer A, Muntel J, Chubukov V, Jules M, Prestel E, Nölker R, et al. Quantitative prediction of genome-wide resource allocation in bacteria. Metab Eng. 2015;32: 232–243.

68. Covert MW, Palsson BØ. Transcriptional Regulation in Constraints-based Metabolic Models of Escherichia coli* 210. Journal of Biological Chemistry. 2002;277: 28058–28064.

69. Covert MW, Palsson BO. Constraints-based models: regulation of gene expression reduces the steady-state solution space. J Theor Biol. 2003;221: 309–325.

70. Covert MW, Schilling CH, Palsson B. Regulation of gene expression in flux balance models of metabolism. J Theor Biol. 2001;213: 73–88.

71. Beard DA, Babson E, Curtis E, Qian H. Thermodynamic constraints for biochemical networks. J Theor Biol. 2004;228: 327–333.

72. Hoppe A, Hoffmann S, Holzhütter H-G. Including metabolite concentrations into flux balance analysis: thermodynamic realizability as a constraint on flux distributions in metabolic networks. BMC Syst Biol. 2007;1: 23. doi:10.1186/1752-0509-1-23

73. Varma A, Palsson BO. Stoichiometric flux balance models quantitatively predict growth and metabolic by-product secretion in wild-type Escherichia coli W3110. Appl Environ Microbiol. 1994;60: 3724–3731.

74. Covert MW, Palsson BØ. Transcriptional Regulation in Constraints-based Metabolic Models of Escherichia coli* 210. Journal of Biological Chemistry. 2002;277: 28058–28064.

75. Covert MW, Schilling CH, Palsson B. Regulation of gene expression in flux balance models of metabolism. J Theor Biol. 2001;213: 73–88.

76. Mahadevan R, Edwards JS, Doyle FJ. Dynamic flux balance analysis of diauxic growth in Escherichia coli. Biophys J. 2002;83: 1331–1340.

77. O'brien EJ, Lerman JA, Chang RL, Hyduke DR, Palsson BØ. Genome-scale models of metabolism and gene expression extend and refine growth phenotype prediction. Mol Syst Biol. 2013;9: 693.

78. O'brien EJ, Lerman JA, Chang RL, Hyduke DR, Palsson BØ. Genome-scale models of metabolism and gene expression extend and refine growth phenotype prediction. Mol Syst Biol. 2013;9: 693.

79. Lerman JA, Hyduke DR, Latif H, Portnoy VA, Lewis NE, Orth JD, et al. In silico method for modelling metabolism and gene product expression at genome scale. Nat Commun. 2012;3: 929.

80. Liu JK, O'Brien EJ, Lerman JA, Zengler K, Palsson BO, Feist AM. Reconstruction and modeling protein translocation and compartmentalization in Escherichia coli at the genome-scale. BMC Syst Biol. 2014;8: 1–15.

81. Mairet F, Gouzé J-L, de Jong H. Optimal proteome allocation and the temperature dependence of microbial growth laws. NPJ Syst Biol Appl. 2021;7: 14. doi:10.1038/s41540-021-00172-y

82. Hui S, Silverman JM, Chen SS, Erickson DW, Basan M, Wang J, et al. Quantitative proteomic analysis reveals a simple strategy of global resource allocation in bacteria. Mol Syst Biol. 2015;11: 784.

83. Basan M, Hui S, Okano H, Zhang Z, Shen Y, Williamson JR, et al. Overflow metabolism in Escherichia coli results from efficient proteome allocation. Nature. 2015;528: 99–104. doi:10.1038/nature15765

84. Scott M, Hwa T. Shaping bacterial gene expression by physiological and proteome allocation constraints. Nat Rev Microbiol. 2023;21: 327–342. doi:10.1038/s41579-022-00818-6

85. González-Hernández Y, Michiels E, Perré P. A Comprehensive Mechanistic Yeast Model Able to Switch Metabolism According to Growth Conditions. Fermentation. 2022;8: 710.

86. Lencastre Fernandes R, Bodla VK, Carlquist M, Heins A-L, Eliasson Lantz A, Sin G, et al. Applying mechanistic models in bioprocess development. Measurement, monitoring, modelling and control of bioprocesses. 2013; 137–166.

87. Hordijk W. Autocatalytic Sets: From the Origin of Life to the Economy. Bioscience. 2013;63: 877–881. doi:10.1525/bio.2013.63.11.6

88. Ameta S, Arsène S, Foulon S, Saudemont B, Clifton BE, Griffiths AD, et al. Darwinian properties and their trade-offs in autocatalytic RNA reaction networks. Nat Commun. 2021;12: 842. doi:10.1038/s41467-021-21000-1

89. Xavier JC, Hordijk W, Kauffman S, Steel M, Martin WF. Autocatalytic chemical networks at the origin of metabolism. Proceedings of the Royal Society B. 2020;287: 20192377.

90. Kayser A, Weber J, Hecht V, Rinas U. Metabolic flux analysis of Escherichia coli in glucose-limited continuous culture. I. Growth-rate-dependent metabolic efficiency at steady state. Microbiology (N Y). 2005;151: 693–706.

Chapter 2 – Proteome Allocation Model of Nutrient Utilization Links Specific Processes to Yield and Maintenance Coefficients

Ohad Golan[1, 2], Uwe Sauer[1§]

[1] Institute of Molecular Systems Biology, ETH Zürich, Otto-Stern-Weg 3, 8093 Zürich, Switzerland

[2] Life Science Zurich PhD Program on Systems Biology, Zurich, Switzerland

Author contributions

OG conceived and designed the study, designed experiments, performed experiments, analyzed data and wrote the manuscript. US wrote the manuscript.

Abstract

We present a coarse-grained proteome allocation model to investigate the cellular processes underlying physiological growth coefficients in microbial cells, with a focus on maintenance and yield. The model qualitatively captures how the growth coefficients are affected by the utilization of different metabolic pathways, including the switch from respiration to partial aerobic fermentation. Our analysis reveals that the maintenance coefficient is influenced not only by the energy expenditures for maintenance processes and the efficiencies of active energy-generating pathways but also the size of non-active proteome sectors. The model is further expanded to include growth on two nutrient sources, a sugar and a biomass precursor such as an amino acid. The model qualitatively predicts the effect of amino acid supplementation on the physiological growth coefficients, providing valuable insights into precursor biosynthesis costs. Overall, our model bridges the gap between physiological measured parameters and cell processes, facilitating the identification of growth-limiting constraints under various conditions.

Introduction

Metabolism constitutes a complex web of interconnected biochemical reactions that transform nutrients into energy and essential cellular components. Understanding the relationship between metabolic processes and cell physiology, including growth rate and biomass yield on different nutrients, is essential for optimizing industrial bioprocesses, combating infectious diseases, and comprehending ecological systems. Nevertheless, the intricate nature of metabolic networks presents considerable challenges in establishing these relationships. Consequently, computational approaches are valuable tools to bridge these gaps and provide a deeper understanding of metabolism.

In this study, we scrutinize the fundamental association between nutrient uptake rate and growth rate. Initial theoretical predictions posited a linear relationship between these factors, where the slope corresponds to the reciprocal of the biomass yield coefficient and the y-

intercept signifies the maintenance coefficient [1,2]. However, this relationship is not universally applicable across diverse growth conditions as demonstrated by empirical data [3–6]. To reconcile this inconsistency, subsequent research introduced a phenomenological modification to the maintenance coefficient, rendering it dependent on the growth rate [7–11]. These alterations were ascribed to variations in metabolic pathways, energy-spilling reactions, and other contributing factors [10,12–14]. However, a definitive connection between specific cellular processes and physiological parameters remains to be established. To tackle this challenge, we introduce a coarse-grained proteome allocation model [15,16] that aims to explore the underlying mechanisms and furnish a more holistic understanding of the interplay between nutrient uptake rate, growth rate, and particular cellular processes.

Our study concentrates on *Escherichia coli* growth on glucose that is known to exhibit a non-linear relationship between uptake and growth rate curves [4]. This non-linearity has been proposed to arise from the activation of the less carbon-efficient aerobic fermentation pathway at high growth rates, a phenomenon referred to as acetate overflow metabolism [4,6]. To substantiate this hypothesis, we evaluate the impact of supplementing amino acids as biomass precursors on the physiological coefficients and compare the onset of the aerobic fermentation pathway activation with the non-linearity in the glucose uptake curve. Subsequently, using our model, we establish connections between physiological coefficients—namely, yield and maintenance—and specific cellular process parameters, including stoichiometric coefficients, proteome sector efficiency, and amino acid biosynthesis costs.

Overall, by establishing connections between physiological parameters and specific cellular process parameters, our results offer a systematic and quantitative framework for elucidating nutrient utilization in *E. coli*. Since the presented methodology can be generalized to other organisms, nutrient availabilities, and stress conditions, it provides a foundation for future investigations of the intricate interplay between metabolism and physiological parameters.

Results

To gain insights into the underlying cellular processes governing nutrient utilization and associated growth coefficients, we characterized the factors influencing the relationship between nutrient uptake rate and growth rate. In continuous cultures this relationship has been theoretically predicted to be linear, as represented by:

$$(1) \qquad J_{in} = m + \frac{1}{Y_k}\lambda$$

where J_{in} refers to the specific nutrient uptake rate per unit biomass, λ denotes the growth rate, m signifies the maintenance coefficient, and Y_k denotes the biomass yield coefficient of nutrient k [1,2,17]. Notably, the biomass yield quantifies the efficiency with which the nutrient contributes to growth, while the maintenance coefficient characterizes the proportion of the nutrient utilized for non-growth-related processes. The latter encompasses all processes that do not directly contribute to an increase in biomass such as energy spilling reactions, motility, macromolecular turnover, or defense against stress [10,13,18–20].

Empirical assessment of nutrient uptake rates across diverse organisms and nutrient sources showed a linear relation for *Aerobacter aerogenes* and *Aerobacter cloacae,* but not for *Selenomonas, Klebsiella aerogenes,* or *E. coli,* which exhibited two distinct linear trends. This finding contradicts conventional theoretical predictions [1,4,5]. This deviation from linearity has been ascribed to alterations in metabolic pathways or growth limiting constraints, as well as a growth rate-dependent maintenance cost [10,21]. To theoretically accommodate this deviation, a phenomenological growth rate-dependent maintenance coefficient has been proposed [7,10,18], but the processes that cause this non-linearity, their connection to the measured physiological coefficients, and the degree to which they influence this relationship remain to be elucidated.

To identify the specific cellular processes impacting the measured physiological coefficients, we determined glucose uptake rates of *E. coli* in batch cultures with glucose as the sole carbon source or glucose supplemented with either the degradable or non-degradable amino acid

aspartate and methionine, respectively [22,23]. Supplementing a non-degradable precursor primarily affects the proteome balance, while a degradable precursor impacts both the proteome and energy balance. Growth rates were modulated by titrating glucose uptake in a strain with an inducible genomic promoter of the transporter encoding gene *ptsG* [24]. Under all conditions, the uptake versus growth rate curve displayed two distinct linear trends, with the second trend exhibiting reduced yield (increased slope) and maintenance (decreased y-intercept) in comparison to the first (fig. 1A). Consistent with expectations [4], the transition to the second, lower yield phase coincided with the onset of acetate secretion (fig. 1B), supporting the hypothesis of a metabolic shift from respiration to partial aerobic fermentation. From these observations we concluded that the active energy generating pathways and availability of biomass precursors influence the yield and maintenance coefficients.

Mathematical model

Driven by the understanding that the physiological coefficients are affected by the active energy generating pathways and the availability of biomass precursors. We therefore aimed to determine how specific cellular parameters, such as the efficiency of the metabolic pathways and the cost of precursor biosynthesis, influence the yield and maintenance coefficients. To associate specific metabolic parameters with the glucose uptake curve, we built upon a previously established coarse-grained proteome allocation model that accurately captures this shift [24]. This model coarse-grains the energy generating pathways of the cell to two pathways: respiration, which fully oxidizes nutrients and is thus more carbon-efficient, and aerobic fermentation, which partially oxidizes nutrients but requires a smaller portion of the proteome, making it less carbon efficient but more proteome-efficient than respiration. At high growth rates, the cell enters a proteome-limited state in which the more proteome-efficient aerobic fermentation pathway that requires much less enzymes than respiration is activated. To represent the glucose uptake curve under different growth conditions, we expanded this model (fig. 2, full mathematical description in Supplementary note 1). Specifically, we divided the growth reaction into a reaction for the biosynthesis of a specific biomass precursor and a

reaction for the remaining growth processes, added reactions for the degradation and uptake of the precursor, and incorporated a growth rate independent maintenance energy demand.

Our expanded model represents a cell that takes in a nutrient source, typically a sugar, at rate J_{in} into metabolite pool x and biomass precursor at rate $J^C_{AS\to A}$ into precursor A metabolite pool. The precursor can be used either for biomass biosynthesis or degraded to metabolite x pool for energy at rate $J^C_{A\to x}$. Metabolite x is utilized in the precursor biosynthesis pathway, the biomass biosynthesis pathway or to generate energy via either the respiration or aerobic fermentation pathways. The carbon flux from metabolite x to respiration, aerobic fermentation, precursor biosynthesis and biomass biosynthesis is denoted by $J^C_{x\to r}$, $J^C_{x\to f}$, $J^C_{x\to A}$ and $J^C_{x\to B}$, respectively.

The energy flux generated via the precursor degradation pathway $J^E_{A\to x}$, respiration $J^E_{x\to r}$ or aerobic fermentation $J^E_{x\to f}$ pathways is used in the pathways for precursor biosynthesis, cell biosynthesis and maintenance, at rates $J^E_{x\to A}$, $J^E_{x\to B}$ and $J^E_{x\to M}$ respectively. The maintenance energy represents energy expenditure and is therefore not correlated with the growth rate. It is important to note that the maintenance energy and maintenance coefficient are two separate terms with the later representing the y-axis intercept of the glucose uptake curve. We partition the overall cell proteome into coarse-grained sectors that facilitate each of the pathways: biomass biosynthesis ($p_{x\to B}$), precursor biosynthesis ($p_{x\to A}$), respiration ($p_{x\to r}$), fermentation ($p_{x\to f}$) and maintenance ($p_{x\to M}$).

The model is based on several key assumptions: (a) **Mass balance and steady state assumption**. The system is in steady state such that the cell components concentrations, i.e., energy, biomass precursor and metabolite x, are constant in time. This assumption is represented by (fig. 2 C-E):

$$J_{in} + J^C_{A\to x} = J^C_{x\to r} + J^C_{x\to f} + J^C_{x\to B} + J^C_{x\to A} \quad (2)$$

$$J^E_{x\to r} + J^E_{x\to f} + J^E_{A\to x} = J^E_{x\to A} + J^E_{x\to B} + J^E_{x\to M} \quad (3)$$

$$J^C_{x\to A} + J^C_{AS\to A} = J^C_{A\to B} + J^C_{A\to x} \quad (4)$$

(b) **Proteome allocation**. The sum of the coarse-grained proteome sectors is equal to one (fig. 2F):

(5) $$p_{x\to f} + p_{x\to r} + p_{x\to B} + p_{x\to A} + p_{A\to x} + p_{x\to M} = 1$$

(c) **Reaction rates.** The rate of a given reaction is linear to the size of the proteome sector processing this reaction as supported by empirical evidence [25]:

(6) $$J^E_{i\to j} = p_{i\to j}\beta_{i\to j}$$

where $J^E_{i\to j}$ is the energy flux of the reaction, $p_{i\to j}$ is the proteome size that executes the pathway and $\beta_{i\to j}$ is a parameter describing the efficiency of the proteome sector. (d) **Set stoichiometry**. The aerobic fermentation and respiration reactions take in carbon from the metabolite x pool as a substrate and produce energy as product. The ratio of carbon to energy is given by:

(7) $$J^E_{x\to r} = \epsilon_{x\to r}J^C_{x\to r}\ ;\ J^E_{x\to f} = \epsilon_{x\to f}J^C_{x\to f}$$

where $\epsilon_{x\to r}$ and $\epsilon_{x\to f}$ are the stoichiometric parameters of the respiration and aerobic fermentation pathways respectively. The stoichiometric relations for carbon to energy in the biosynthesis and degradation of the biomass precursor are:

(8) $$J^E_{x\to A} = \epsilon_{x\to A}J^C_{x\to A};\ J^E_{A\to x} = \epsilon_{A\to x}J^C_{A\to x}$$

where $\epsilon_{x\to A}$ and $\epsilon_{A\to x}$ are the stoichiometric parameters of the biosynthesis and degradation of the biomass precursor pathways respectively. (e) **Growth rate demands**. The cell biosynthesis proteome fraction $p_{x\to B}$ under carbon limitation follows a linear growth rate dependence [24–27]:

(9) $$p_{x\to B} = p_0 + \sigma_{x\to B}\lambda$$

The cell biosynthesis rate is proportional to the flux of the necessary growth components (energy, carbon, and biomass precursor) according to a fixed stoichiometry of the metabolic network [28,29]:

(10) $J^E_{x\to B} = \sigma_E\lambda$; $J^C_{x\to B} = \sigma_C\lambda$; $J^C_{A\to B} = \sigma_A\lambda$

(f) **Maintenance energy.** The demand is constant and independent of the growth rate:

(11) $J^E_{x\to M} = E_M$

any maintenance energy that is proportional to the growth rate is coarse-grained into the cell biosynthesis reaction.

The difference in efficiencies of the two energy-generating pathways, respiration and fermentation, is represented in the metabolic stoichiometry and proteome efficiency parameters. Respiration has a higher carbon efficiency, meaning it generates more energy per carbon compared to aerobic fermentation [30]. This is reflected in the stoichiometric parameters describing the energy generated per carbon unit $\epsilon_{x\to r} > \epsilon_{x\to f}$ (According to [24]: $\epsilon_{x\to r} = 4.2\,\frac{ATP}{carbon}$, $\epsilon_{x\to f} = 2\,\frac{ATP}{carbon}$). On the other hand, aerobic fermentation is more proteome efficient [24,31–33], meaning it generates more energy per proteome fraction than respiration. This is reflected in the proteome efficiency parameters describing the energy generated per proteome unit $\beta_{x\to f} > \beta_{x\to r}$ (Measured by [24]: $\beta_{x\to r} = 390\,\frac{mM\ ATP}{OD_{600}h}$, $\beta_{x\to f} = 750\,\frac{mM\ ATP}{OD_{600}h}$).

Growth on a single nutrient source

To ascertain whether our model successfully captures the transition from respiration to partial aerobic fermentation, we first predicted growth on a single nutrient source. In this scenario, there is no uptake flux of the biomass precursor, meaning $J^C_{AS\to A} = 0$, and the cell is tasked with synthesizing all necessary precursors for growth (fig. 2A). We assume that no futile cycle occurs involving the degradation and biosynthesis of the biomass precursor, setting $p_{A\to x} = J^C_{A\to x} = 0$. The acetate secretion rate is determined by the flux through the aerobic fermentation pathway given by $J_{ac} = S_{ac}J^C_{x\to f}$, where S_{ac} being determined by the involved stoichiometry. Solving eqs. 3-11 for acetate secretion gives an acetate secretion rate that increases linearly with the growth rate (fig. 3B, solid brown curve):

(12) $$J_{ac}(single\ nutrient) = \frac{S_{ac}}{\epsilon_{x\to f}}\left(p''_E\beta_E - \lambda\left(\sigma_{x\to B} + \frac{\sigma_E}{\beta_{x\to r}} + \sigma_A\epsilon_{x\to A}\left(\frac{1}{\beta_{x\to r}} + \frac{1}{\beta_{x\to A}}\right)\right)\beta_E\right)$$

where $\beta_E = \frac{\beta_{x\to f}\beta_{x\to r}}{\beta_{x\to r}-\beta_{x\to f}}$ and $p''_E = p_E - E_M\left(\frac{1}{\beta_{x\to M}} + \frac{1}{\beta_{x\to r}}\right)$. As the aerobic fermentation pathway is more proteome efficient, β_E has a negative value, resulting in a positive slope and a negative y-intercept, providing a good fit to the experimental data (compare solid brown curve in fig. 3B to blue curve fig. 1B). Since negative acetate secretion is not feasible, the model predicts that the growth rate for onset of acetate secretion, λ_{ac}, occurs when $J_{ac} = 0$:

(13) $$\lambda_{ac} = \frac{p''_E}{\sigma_{x\to B} + \frac{\sigma_E}{\beta_{x\to r}} + \sigma_A\epsilon_{x\to A}\left(\frac{1}{\beta_{x\to r}} + \frac{1}{\beta_{x\to A}}\right)}$$

At growth rates below the onset of acetate secretion, there is no flux through the aerobic fermentation pathway, so the aerobic fermentation proteome sector size is zero: $p_{x\to f}(\lambda < \lambda_{ac}) = 0$. Thus, the model captures the acetate secretion curve.

To explore the model's solution for the glucose uptake curve, we split the solution into two regimes based on whether the growth rate is above or below the onset of acetate secretion. For growth rates above the onset of acetate secretion where the aerobic fermentation pathway is active, combining eqs. 2-11 gives (fig. 3A, solid brown curve):

(14) $$J_{in}\ (single\ nutrient, \lambda > \lambda_{ac}) = \frac{\beta_E}{\epsilon_E}p''_E + \frac{E_M}{\epsilon_{x\to r}} + \lambda\left(\sigma_C + \frac{\sigma_E}{\epsilon_{x\to r}} + \sigma'_A - \sigma_A^r - \left(\sigma_{x\to B} + \frac{\sigma_E}{\beta_{x\to r}}\right)\frac{\beta_E}{\epsilon_E}\right)$$

where $\epsilon_E = \frac{\epsilon_{x\to f}\epsilon_{x\to r}}{\epsilon_{x\to r}-\epsilon_{x\to f}}$, $\sigma'_A = \sigma_A\left(1 + \frac{\epsilon_{x\to A}}{\epsilon_{x\to r}}\right)$, and $\sigma_A^r = \sigma_A\frac{\beta_E}{\epsilon_E}\left(\epsilon_{x\to A}\left(\frac{1}{\beta_{x\to r}} + \frac{1}{\beta_{x\to A}}\right)\right)$. This solution yields a linear curve with a positive slope representing the theoretical reciprocal of the yield coefficient $\frac{1}{Y_{theo}}(single\ nutrient, \lambda > \lambda_{ac}) = \left(\sigma_C + \frac{\sigma_E}{\epsilon_{x\to r}} + \sigma'_A - \left(\sigma_{x\to B} + \frac{\sigma_E}{\beta_{x\to r}}\right)\frac{\beta_E}{\epsilon_E}\right)$, and a y-intercept representing the theoretical maintenance coefficient $m_{theo}(single\ nutrient, \lambda > \lambda_{ac}) = \frac{\beta_E}{\epsilon_E}p''_E + \frac{E_M}{\epsilon_{x\to r}}$.

Upon extrapolation to zero growth, in this growth rate range, the model would predict a maintenance coefficient that could potentially be negative, contradicting the interpretation of this coefficient as nutrient flux utilized for non-growth-related processes. Instead, the model shows this coefficient is composed of the combined non-growth correlated energy and proteome costs normalized by their efficiencies. A linear fit to the experimental results in this range (fig. 1A, blue curve) indeed yields a negative value (fig. 4A, blue bar), but the large measurement error renders it inconclusive. Previous measurements reported a maintenance coefficient of $-0.0012\frac{mM}{gdw\,h}$ for *Aerobacter aerogenes* [6] or $-7.9\,\frac{mM}{gdw\,h}$ for *Schizosaccharomyces pombe* [21] in glucose-limited culture which demonstrates a good qualitative fit to the negative theoretical prediction. Moreover, eq. 15 shows that the maintenance coefficient is a factor of not only the maintenance energy E_M, but is also highly dependent on the energy pathways efficiency parameters ($\epsilon_{x\to r}$, $\epsilon_{x\to f}$, $\beta_{x\to r}$, $\beta_{x\to f}$) and the non-growth-related proteome sector (p_E).

For growth rates below the onset of acetate secretion, where the aerobic fermentation pathway is inactive, the model encounters more constraints than parameters, resulting in three possible solutions. Each of these solutions neglects one of the three governing equations (carbon balance, energy balance, or proteome allocation) as only two can be effective simultaneously. The first solution is carbon sufficient growth, which neglects the carbon balance constraint (eq. 2) and relies on the constraints for the energy balance (eq. 3) and proteome allocation (eq. 5). This solution produces (fig. 3A, black dashed curve):

$$\lambda = \frac{p''_E}{\sigma_{x\to B} + \frac{\sigma_E}{\beta_{x\to r}} + \sigma_A \epsilon_{x\to A}\left(\frac{1}{\beta_{x\to r}} + \frac{1}{\beta_{x\to A}}\right)} \quad (15)$$

However, we dismiss this solution, as it predicts a constant growth rate independent of nutrient uptake rate, which contradicts the experimental evidence showing a strong correlation between the two factors. The second solution is energy-limited growth, considering both the carbon and energy constraints but disregarding the proteome allocation constraint (eq. 5). This solution yields (fig. 3A, solid red curve):

(16) $$J_{in}\ (single\ nutrient, \lambda < \lambda_{ac}) = \frac{E_M}{\epsilon_{x\to r}} + \left(\sigma_C + \frac{\sigma_E}{\epsilon_{x\to r}} + \sigma'_A\right)\lambda$$

Lastly, the third solution is proteome-limited growth, which is based on the carbon balance (eq. 2) and proteome allocation (eq. 5) constraints but disregards the energy balance constraint (eq. 3). This solution produces (fig. 3A, blue curve):

(17) $$J_{in}\ (single\ nutrient, \lambda < \lambda_{ac}) = \frac{\beta_{x\to r}}{\epsilon_{x\to r}}\ (p_E - \frac{E_M}{\beta_{x\to M}}) + \left(\sigma_C - \frac{\beta_{x\to r}}{\epsilon_{x\to r}}\sigma_{x\to B} + \sigma'_A - \frac{\epsilon_{x\to A}}{\epsilon_{x\to r}}\sigma_A^p\right)\lambda$$

where $\sigma_A^p = \sigma_A\left(1 + \frac{\beta_{x\to r}}{\beta_{x\to A}}\right)$. Both the energy-limited and proteome-limited solutions expressed in eqs. 17-18 predict a linear solution with a positive slope and y-intercept (see supplementary note 1 for parameter value assessment).

The above model analysis relates specific cellular processes to the physiological coefficients of maintenance energy and biomass yield. Below the onset of acetate secretion, it is unclear whether cell growth is limited by energy or proteome. To differentiate, we compared the theoretical physiological coefficients to the measured ones (fig. 4C-D, compare blue bar to stroked bars). The reciprocal of the yield coefficient (the slope of the glucose uptake to growth rate) shows a slightly better fit to the theoretical solution for energy-limited than proteome-limited growth but the large error renders this inconclusive (fig. 4D). The measured maintenance parameter shows a better fit to energy-limited compared to proteome-limited growth. Previous measurements of the maintenance coefficient for *E. coli* strain ML308 data reported a value of $0.09\frac{mmol\ carbon}{OD_{600}h}$ [3] which also gives a better fit to the values predicted for energy-limited growth.

Theoretically, two limitation scenarios could govern *E. coli* physiology at growth rates below the onset of acetate secretion, of which the experimental data support the energy-limited scenario. A key question arises: what occurs when the growth rate increases, and the energy-limited solution intersects with the proteome-limited solution? Do cells experience a transition to exclusively proteome-limited growth at a specific growth rate? To explore this, we first investigated the specific growth rate at which this intersection occurs. By equating the two

solutions (eqs. 17 and 18), we calculated the growth rate where the energy-limited and proteome-limited solutions intersect. Intriguingly, this intersection happens at the same growth rate λ_{ac} as the onset of acetate secretion, after which the cell activates the more proteome efficient aerobic fermentation pathway. Previous studies demonstrated that the activation of the partial aerobic fermentation pathway at high growth rates is a programmed global response used by cells to balance the conflicting proteomic demands of energy biogenesis and biomass synthesis for rapid growth [24]. Here, we offer a supplementary perspective where the model predicts a metabolic switch at the intersect of the energy and proteome limited solutions without prior information about the fermentation pathway. The observed switch to partial aerobic fermentation fits this prediction.

Growth on dual nutrient sources: sugar and biomass precursor

To further test the model, we considered the amino acid supplementation experiments (fig. 1) that perturbed energy and proteome resources by alleviating the need for their biosynthesis (fig. 3B). The degradable amino acid aspartate can both be catabolized and used directly for biosynthesis, thus may affect both the energy and proteome balance. The non-degradable amino acid methionine, in contrast, can only be utilized for biosynthesis and therefore affects primarily the proteome balance.

To accommodate the model to supplementation of the non-degradable methionine, the degradation flux and the corresponding proteome sector were set to zero: $J_{A\to x} = p_{A\to x} = 0$. Furthermore, we assume that due to the high concentration of the precursor in the growth medium and its low uptake cost compared to biosynthesis, the cell acquires it solely through uptake and does not engage in its biosynthesis. As a result, the precursor biosynthesis flux and the corresponding proteome sector are also set to zero: $J^{C}_{x\to A} = p_{x\to A} = 0$. Under these conditions, by solving eqs. 3-11, the model predicts the following acetate secretion curve (fig. 3B, dashed brown curve) and growth rate for onset of acetate secretion:

$$(18) \qquad J_{ac}\,(non-degradable) = \frac{S_{ac}}{\epsilon_{x\to f}}\left(p''_{E}\beta_{\mathrm{E}} - \lambda\left(\sigma_{x\to B} + \frac{\sigma_E}{\beta_{x\to r}}\right)\beta_{\mathrm{E}}\right)$$

(19) $\lambda_{ac}(non-degradable) = \frac{p''_E}{\sigma_{x\to B}+\frac{\sigma_E}{\beta_{x\to r}}}$.

To assess the impact of precursor supplementation, we compared the model predictions for growth with and without the precursor by subtracting the respective solutions. The effect on the acetate secretion curve is a decrease in slope without affecting the y-intercept, demonstrated by the following equation (subtract eq. 18 from eq. 12):

(20) $J_{ac}(non-degradable) - J_{ac}(single\ nutrient) = \frac{S_{ac}}{\epsilon_{x\to f}}\beta_E\left(\sigma_A\epsilon_{x\to A}\left(\frac{1}{\beta_{x\to A}}+\frac{1}{\beta_{x\to r}}\right)\right)\lambda$

Eq. 20 reveals the specific parameters that influence the shift in the slope, such as the proteome and carbon efficiencies of the biomass precursor biosynthesis pathway, as well as the demand for the biomass precursor for growth. Linear fits to the acetate secretion curves show that the addition of methionine does not affect the y-intercept of the acetate secretion curve, consistent with the model prediction (Supplementary fig. 1). The slope of the acetate secretion curve of the methionine curve was smaller than that of growth on glucose alone as predicted, though not significantly (Supplementary fig. 1). However, the onset of acetate secretion with methionine was clearly higher for growth with methionine (see Figure 1B, compare blue and black curves), as predicted (see Supplementary note 1, eq. S73).

The glucose uptake curve is again divided into two regions, below and above the onset of acetate secretion. For growth rates above the onset of acetate secretion, the aerobic fermentation pathway is active ($J^C_{x\to f} > 0$). Combining eqs. 2-11 with the constraints for this growth rate region, we obtain:

(21) $J_{in}\ (non-degradable, \lambda > \lambda_{ac}) = \frac{\beta_E}{\epsilon_E}p''_E + \frac{E_M}{\epsilon_{x\to r}} + \left(\sigma_C + \frac{\sigma_E}{\epsilon_{x\to r}} - \left(\sigma_{x\to B} + \frac{\sigma_E}{\beta_{x\to r}}\right)\frac{\beta_E}{\epsilon_E}\right)\lambda$.

Similar to the solution for growth on a single nutrient source, the model predicts a linear curve with a positive slope (reciprocal of the yield) $\frac{1}{Y_{theo}}(non-degradable, \lambda > \lambda_{ac}) = \sigma_C + \frac{\sigma_E}{\epsilon_{x\to r}} - \left(\sigma_{x\to B} + \frac{\sigma_E}{\beta_{x\to r}}\right)\frac{\beta_E}{\epsilon_E}$. However, a negative maintenance coefficient (the y-intercept) $m_{theo}(non-$

$degradable, \lambda > \lambda_{ac}) = \frac{\beta_E}{\epsilon_E} p''_E + \frac{E_M}{\epsilon_{x\to r}}$. The experimental results show a good qualitative fit to these predictions (fig. 4A-B, black bar).

The effect of a non-degradable biomass precursor on the glucose uptake curve in this range as depicted by the difference in the curves gives (subtract eq. 21 from eq. 14):

(22) $$J_{in}\ (non-degradable, \lambda > \lambda_{ac}) - J_{in}\ (single\ nutrient, \lambda > \lambda_{ac}) = \lambda\sigma_A\epsilon_{x\to A}\left(\frac{\beta_E}{\epsilon_E}\left(\frac{1}{\beta_{x\to A}} + \frac{1}{\beta_{x\to r}}\right) - \left(\frac{1}{\epsilon_{x\to A}} + \frac{1}{\epsilon_{x\to r}}\right)\right).$$

Eq. 22 shows that addition of a non-degradable precursor is predicted to have no effect on the maintenance coefficient (the y-intercept doesn't change) but increases the yield (decrease the slope of the curve). The experimental data indeed shows an increased yield and a maintenance coefficient within this range (fig. 4A-B, compare blue and black bars).

For growth rates below the onset of acetate secretion, the aerobic fermentation pathway is inactive ($J^C_{x\to f} = 0$) and as in the case for growth on a single nutrient source there are three solutions. The carbon sufficient solution neglects the carbon balance constraint (eq. 2) and is based on the energy balance (eq. 3) and proteome allocation (eq. 5) constraints. This solution yields (fig 3A, dashed grey line):

(23) $$\lambda = \frac{p''_E}{\sigma_{x\to B} + \frac{\sigma_E}{\beta_{x\to r}}}.$$

This solution gives a constant growth rate which does not fit the experimental results of correlation between the growth rate and nutrient uptake rate. The energy-limited growth solution considers both the carbon (eq. 2) and energy (eq. 3) balance constraints but disregards the proteome allocation constraint (eq. 5). This solution yields (fig. 3A, dashed red curve):

(24) $$J_{in}\ (non-degradable, \lambda < \lambda_{ac}) = \frac{E_M}{\epsilon_{x\to r}} + \left(\sigma_C + \frac{\sigma_E}{\epsilon_{x\to r}}\right)\lambda.$$

The proteome-limited growth solution considers both the carbon (eq. 2) and energy balance constraints (eq. 3) but disregards the proteome allocation constraint (eq. 5). This solution results in a curve (fig. 3A, dashed blue curve) given by:

$$(25) \qquad J_{in}\ (non-degradable, \lambda < \lambda_{ac}) = \frac{\beta_{x\to r}}{\epsilon_{x\to r}}\left(p_E - \frac{E_M}{\beta_{x\to M}}\right) + \left(\sigma_C - \sigma_{x\to B}\frac{\beta_{x\to r}}{\epsilon_{x\to r}}\right)\lambda.$$

Both the energy- and proteome-limited solutions give a linear curve with reciprocal of yield coefficient of $\frac{1}{Y_{theo}^{ene}}(non-degradable, \lambda < \lambda_{ac}) = \left(\sigma_C + \frac{\sigma_E}{\epsilon_{x\to r}}\right)$ and $\frac{1}{Y_{theo}^{prot}}(non-degradable, \lambda < \lambda_{ac}) = \left(\sigma_C - \sigma_{x\to B}\frac{\beta_{x\to r}}{\epsilon_{x\to r}}\right)$, and a maintenance coefficient of $m_{theo}^{ene}(non-degradable, \lambda < \lambda_{ac}) = \frac{E_M}{\epsilon_{x\to r}}$ and $m_{theo}^{prot}(non-degradable, \lambda < \lambda_{ac}) = \frac{\beta_{x\to r}}{\epsilon_{x\to r}}\left(p_E - \frac{E_M}{\beta_{x\to M}}\right)$ for the energy-limited and proteome-limited solutions, respectively.

The effect of a non-degradable biomass precursor on the glucose uptake curve, as depicted by the difference in the curves, is as follows. For the energy-limited solution (subtract eq. 24 from eq. 16):

$$(26) \qquad J_{in}\ (non-degradable, \lambda < \lambda_{ac}) - J_{in}\ (single\ nutrient, \lambda < \lambda_{ac}) = -\sigma_A\left(1 + \frac{\epsilon_{x\to A}}{\epsilon_{x\to r}}\right)\lambda$$

and for the proteome-limited solution (subtract eq. 25 from 17):

$$J_{in}\ (non-degradable, \lambda < \lambda_{ac}) - J_{in}\ (single\ nutrient, \lambda < \lambda_{ac}) = -\sigma_A\left(1 - \frac{\epsilon_{x\to A}}{\epsilon_{x\to r}}\frac{\beta_{x\to r}}{\beta_{x\to A}}\right)\lambda.$$

For both limitations, the addition of the biomass precursor is expected to increase the yield (reduce slope) without affecting the maintenance coefficient (the y-intercept).

The maintenance coefficient comparison for growth with and without methionine showed no significant difference, as predicted by the model, although there were high measurement errors (fig 4.C). The difference in slope for growth with and without methionine represents the reduced proteome and energy costs for methionine biosynthesis. The varying results for growth rates below and above the onset of acetate secretion (fig 4. B,D) indicate that this cost depends on the active metabolic pathways, consistent with the model's predictions. The disparity in yield

between growth with methionine and growth without methionine is more pronounced in the growth range below the onset of fermentation, indicating a higher cost associated with its biosynthesis in this range.

To investigate the more complicated case of growth with the degradable biomass precursor aspartate that can be used for both biosynthesis and energy generation, we made the following assumptions. Similar to a non-degradable precursor, we assume that uptake is preferred over biosynthesis, such that $J^C_{x\to A} = p_{x\to A} = 0$. Since, in this case, the precursor can be degraded back to the metabolite x pool, we add a free parameter to the model to include that possibility. Assuming that the uptake rate of the precursor $J^C_{AS\to A}$ is linear to the growth rate in each growth region in the form $J^C_{AS\to A} = \xi_0 + \xi_{AS\to A}\lambda$, determining the parameters ξ_0 and $\xi_{AS\to A}$ will also establish how the precursor is utilized by the cell. For example, $\xi_0 = 0$ would indicate that the precursor is used only for cell biosynthesis and not degraded (full model solution in supplementary note 1). Comparison of the linear fits of the glucose uptake curve with supplementation of aspartate (fig. 1A, red curves) to that with growth only on glucose (fig. 1A, blue curves) revealed that aspartate affected both the maintenance and yield in both growth regions (fig. 4). The shift in the maintenance coefficient indicates that indeed some fraction of aspartate was degraded rather than utilized for cell biosynthesis. Surprisingly, aspartate decreased both the maintenance coefficient and the yield (increased the slope) at growth rates above the onset of acetate secretion (fig. 4A-B). This suggests a possible tradeoff in the utilization of aspartate between decreasing maintenance and increasing the yield of the utilized sugar.

Discussion

Understanding the connections between metabolic processes and cell physiology has been a challenge for scientists for over a century. In this study, we develop a systematic and quantitative framework for understanding nutrient utilization in bacterial growth. We focus on two primary physiological parameters, the maintenance and yield coefficients in *E. coli*. Using a proteome allocation model that incorporates the proteome, energy and carbon constraints,

we show how the growth coefficients are affected by the utilization of distinct metabolic pathways, specifically respiration and aerobic fermentation. Our analysis shows that the maintenance coefficient is influenced by not only the energy expenditures for maintenance processes and the efficiencies of active energy-generating pathways, but also the non-active proteome sectors. Thus, we provide a quantitative framework capable of discerning the impact of various growth-limiting constraints and key cellular parameters on physiological growth coefficients. Leveraging this framework, we introduce a measure to assess the cost of precursor biosynthesis.

Previous studies attempted to connect metabolic processes and cell physiology by integrating the molecular constituents of cells into a genome-scale models [4,34–38]. While such models can be useful in predicting emergent phenotypes, they are difficult to construct and maintain, require kinetic parameters that are not readily available [39], and their complexity makes it hard to relate specific cell processes to the physiological parameters. Other models were either exclusively phenomenological [40,41] or focused solely on stoichiometry, overlooking proteome costs [40,42]. Alternative models accounted for the proteome cost associated with precursor biosynthesis but neglected the energy flux balance within the cell, disregarding the energetic expenditures for precursor and cellular biosynthesis, as well as energy-generating pathways [43]. In this study, we expand upon prior coarse-grained proteome allocation models[24–27] to encompass stoichiometry, energy balance, and proteome costs, offering a more comprehensive perspective.

The concept of maintenance expenditures is complex and has been a long-standing subject of debate [10]. It has been attributed to various cellular processes such as cell motility, osmoregulation, turnover of macromolecular compounds, defense against stress, energy spilling, and extracellular losses of compounds [10,12,13,18]. Although the physiological maintenance coefficient in continuous culture has been described phenomenologically, the direct effect of specific cell processes has not been linked to it. In our study, we differentiate between the maintenance coefficient, defined as the y-axis intercept of the glucose uptake

curve, and maintenance energy, which encapsulates all non-growth-rate-correlated energy expenditures of the cell. Our analysis reveals that the maintenance coefficient depends not only on the maintenance energy and the efficiencies of active energy generating pathways, as been preciously suggested [44], but also on the non-active proteome sectors. We focus on the shift from respiration metabolism to fermentation to demonstrate that this change in metabolic pathway utilization can indeed affect the maintenance coefficient. Furthermore, when multiple energy generating pathways are active, the maintenance coefficient can be negative, contradicting the interpretation of the maintenance coefficient as nutrient utilized for non-growth-related purposes. It is important to note that the biological significance of this coefficient should not be interpreted as nutrient utilization at zero growth rate, as this extrapolation leads to an unrealistic scenario in which cells secrete nutrients. Instead, it should be considered as a valuable measurable parameter that provides abundant information about growth limiting constraints and nutrient utilization preferences as demonstrated here for the case of growth with supplementation of aspartate.

In the field of metabolic engineering, efforts are often focused on maximizing the production of valuable by-products. As part of this process, the yield and maintenance coefficients serve as practical proxies for understanding the effects of genetic modifications on cellular processes [44,45]. Typically, strategies aim to increase the yield and reduce the maintenance coefficient as measured for the growth range below the onset of fermentation. However, it is crucial to note that these coefficients might not always be the most pertinent parameters in all scenarios. Specifically, many bioproduct formation processes occur during the fermentation range [44,45]. Our analysis reveals that in this range, the yield and maintenance coefficients are also influenced by parameters other than the ones observed below the onset of fermentation, such as the proteome efficiencies of the various pathways. Furthermore, the effect of the different parameters is not always trivial. For example, our analysis predicts that improving the proteome efficiency of the respiration pathway could potentially decrease the maintenance coefficient (to a higher negative value) but also decrease the yield in the fermentation range (supplementary fig. 2).

At growth rates below the onset of fermentation, our analysis indicates that multiple model solutions can arise depending on the specific constraints considered – namely, carbon sufficient, energy-limited, or proteome-limited growth. By fitting experimental data to the model, we propose that for respiratory growth of *E. coli* under glucose-limited conditions, growth is predominantly energy-limited. Whether purely proteome-limited growth occurs under certain conditions remains an open question. Previous research has proposed that that the growth limiting substrate depends on the nutrient's degree of reduction such that lowly reduced nutrient lead to energy-limited growth while highly reduced nutrients result in carbon limited growth [46]. Our model predicts that carbon limitation always coincides with either proteome or energy limitation, as both energy- and proteome-limited growth solutions incorporate the carbon balance assumption. Instead, we speculate that growth in highly reduced nutrients leads to proteome-limited growth. Alternatively, proteome-limited growth might occur under high-stress conditions such as those experienced in high heat or under antibiotic treatment that necessitate substantial proteome investment.

An important question in evolutionary biology and biotechnology are the cost for precursor biosynthesis [47]. Previous studies have calculated these costs based on either the energetic costs involved in precursor biosynthesis [48–53] or the proteome cost associated with the precursor biosynthesis pathway [54]. In this study, we suggest using the shift in maintenance and yield coefficients as a proxy for the comprehensive cost of biomass precursor biosynthesis, encompassing both energetic and proteomic costs. By utilizing our model, we were able to identify which growth parameters affect the coefficients and predict that the cost of amino acid biosynthesis varies under different growth modes, such as respiratory and partial aerobic fermentation [55]. This approach holds the potential to clarify deviations from the theoretical predicted trend of amino acid usage abundance to cost of biosynthesis as measured only by the energetic cost [47,56] or proteome cost [54] in yeast, or deviations from expected uptake of amino acids according to cost in *E. coli* [57]. Our previous research demonstrated that amino acids utilization efficiency in batch culture is affected by the availability and the relative amounts of other nutrients, deviating from the theoretical prediction

based on the sum of nutrient dissipation energies [58]. Our current analysis proposes that this deviation could potentially result from the effect of proteome allocation on yield, a factor not included in the model of the previous study.

Our coarse-grained proteome allocation model offers a comprehensive framework for understanding nutrient utilization; however, it is essential to acknowledge that it does not account for all possible constraints impacting cellular metabolism. Factors such as molecular and membrane crowding, as well as the effects of different stresses such as pH, temperature, and oxidative stress are not explicitly included in the model. For example, intracellular and membrane crowding [59–63], which has been proposed as the growth-limiting constraint at high growth rates in yeast [21], is not considered in our analysis. Moreover, the assumptions of the model may not hold true in extremely low nutrient concentrations. Under these conditions, metabolic pathway flux may no longer exhibit a linear relation with the proteome sector due to low substrate concentrations. An alternative definition of maintenance considers it as the minimal energy required to sustain the organism during starvation [10,64,65]. Values measured according to this definition do not fit the values measured according to the intercept with the y-axis of the nutrient uptake curve [65]. Our model cannot predict the maintenance in this range as it does not hold in low nutrient concentrations or under starvation. Nevertheless, our model provides a framework that can be adapted to accommodate these additional constraints and complexities. Future work can focus on incorporating these factors into the model to enhance its accuracy and applicability.

Our study provides valuable insights into the underlying cellular processes that govern nutrient utilization and the associated growth coefficients, which have implications for both evolutionary biology [11,66] and biotechnology [67–69]. Our coarse-grained proteome allocation model serves as a starting point for further investigation and development of more comprehensive models that account for additional constraints and stress factors. For instance, extending the model to account for challenging environments, such as those encountered during antibiotic treatment, could potentially reveal proteome trade-offs cells are forced to make, enabling the

identification of strategies for optimizing antibiotic therapy to target specific bacterial vulnerabilities and minimize the risk of resistance development.

Material and methods

Data analysis:

The OD measured by the microplate reader was linearized using a premeasured calibration curve. Growth curves obtained in the microplate reader were compared to growth curves obtained in shake flask and were equivalent. All linear fits were done to the average of the triplicate measurements by method of least-mean-square [70].

Strains and growth essays:

In the growth essays the NQ1243 [24] was used. The experiment was done at 37ºC shaker shaking at 350 rpm in three steps: seed culture, pre-culture and experimental culture. For seed culture, one colony from fresh LB agar plate was inoculated into test tube with M9 minimal medium with 4 gr/l glucose and cultured in 37ºC shaking at 350 rpm for 8-9 hours. The culture was then diluted in pre-warmed 96 deep well plate to an OD_{600} of 0.05-0.4 so that all cultures reached exponential phase at the same time. Each growth condition in the deep well plate was run in triplicates. All conditions contained m9 minimal medium, 4 gr/l glucose and different concentrations of the inducer for the glucose uptake promoter 3methyl-benzyl. The growth conditions with methionine or aspartate contained 0.1 gr/l methionine or 1 gr/l aspartate respectively. Every 30 min, 40 µl culture from every well were collected and used to measure OD_{600} using Tecan microplate reader (Tecan Infinite M200). Another 100 µl culture from every well was collected, centrifuged at 15,000 rpm, the supernatant was collected and immediately frozen.

Supernatant were used to measure acetate concentrations using Acetate assay kit (Megazyme Acetic Acid Assay Kit) amd glucose concentrations using D-Glucose Assay Kit (Gopod format). The slope of the plot of acetate/glucose concentrations versus OD_{600} for all

replicates (multiplied with the measured growth rate) was used to determine the acetate secretion/glucose uptake rate.

Supplementary material

All supplementary material is available on: https://doi.org/10.5281/zenodo.8359139 .

Acknowledgments

OGo and US acknowledge support by Marie Skłodowska-Curie Actions ITN “SynCrop” (grant agreement no. 764591). Figures were generated using Biorender.

We are grateful to H. de Jong and A. Y. Weiße for valuable discussion and comments.

Figures

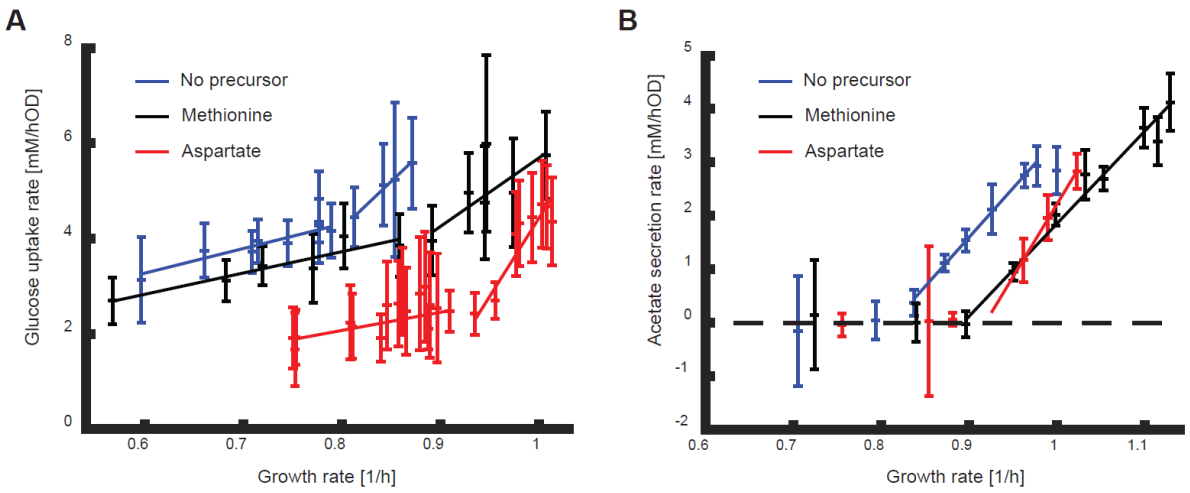

Figure 1 – Physiological growth coefficients of growth in different conditions. (A-B) Glucose uptake and acetate secretion rates as function of growth rate for growth without supplementation of a biomass precursor and supplementation of methionine or aspartate. Curves show linear fit region (fit parameter R2>0.9). Error bars depict error of fit parameter.

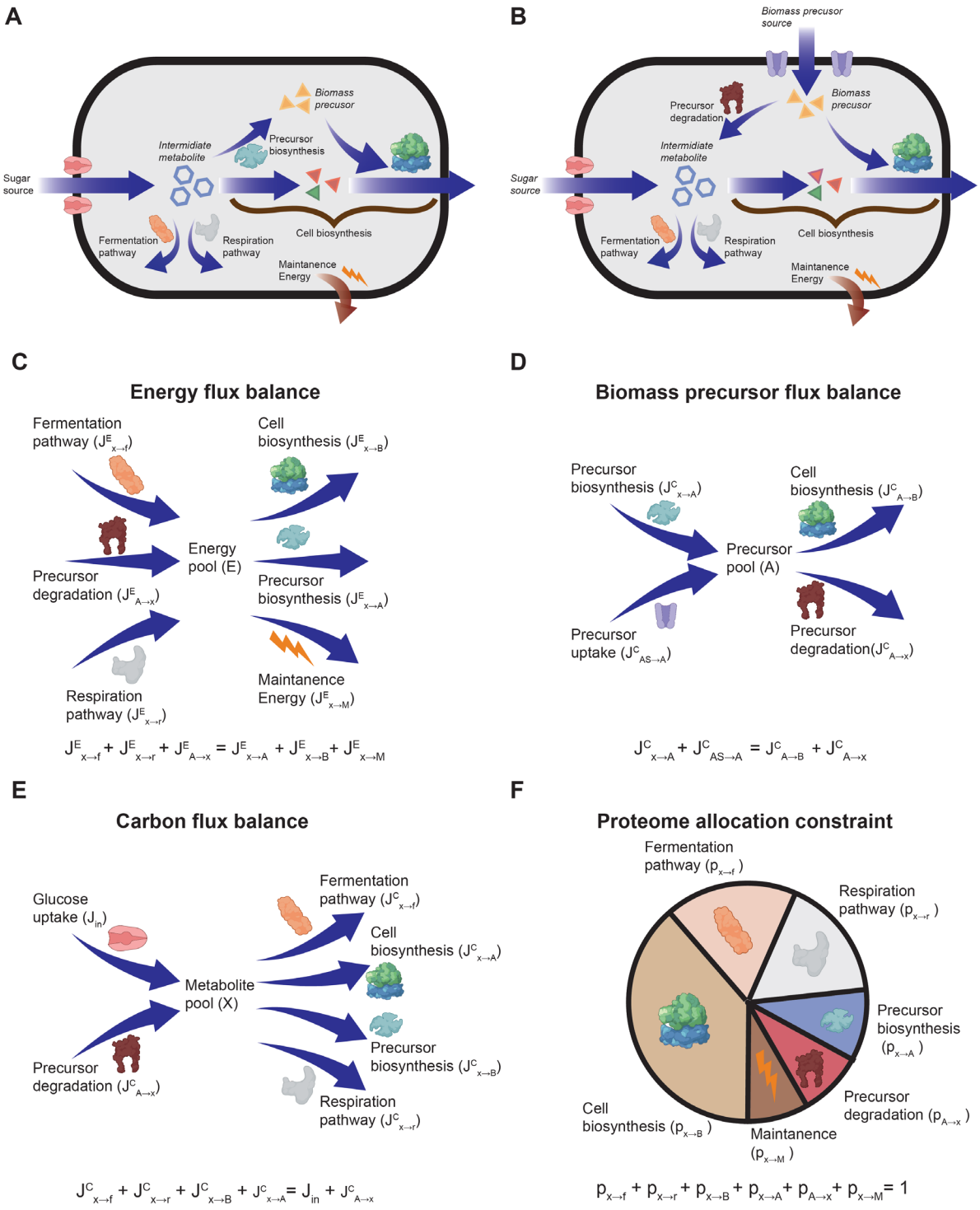

Figure 2 – Mathematical model for growth on a single nutrient source. (A) Model schematics. The cell takes in some sugar into metabolite x pool. Metabolite x is used to generate energy via the respiration or aerobic fermentation pathways, to biosynthesize the biomass precursor or for cell biosynthesis. **(B)** With availability of a biomass precursor source, the cell no longer needs to biosynthesize the precursor and is also able to degrade it back to

an intermediate metabolite. **(C)** Energy flux balance. The energy generated in the respiration ($J^E_{x\to r}$) and fermentation ($J^E_{x\to f}$) pathways is used for cell biosynthesis ($J^E_{x\to B}$), precursor biosynthesis ($J^E_{x\to A}$) and maintenance ($J^E_{x\to M}$). **(D)** Precursor flux balance. The precursor coming in from uptake ($J^C_{AS\to A}$) and biosynthesis ($J^C_{x\to A}$) is utilized in the precursor degradation ($J^C_{A\to x}$) and biomass biosynthesis pathways ($J^C_{x\to B}$). **(E)** Carbon flux balance. The carbon coming in from the uptake of the nutrient (J_{in}) and degradation of the precursor ($J^C_{A\to x}$) is utilized to generate energy via either the respiration ($J^C_{x\to r}$) and aerobic fermentation ($J^C_{x\to f}$) pathways, for precursor biosynthesis ($J^C_{x\to A}$) or for biomass biosynthesis ($J^C_{x\to B}$). **(F)** Proteome allocation constraint. The proteome is distributed to the different proteome sectors: Energy generation via the respiration ($p_{x\to r}$) or aerobic fermentation ($p_{x\to f}$) pathways, precursor biosynthesis ($p_{x\to A}$), precursor degradation ($p_{A\to x}$), cell biosynthesis ($p_{x\to B}$) or maintenance ($p_{x\to M}$).

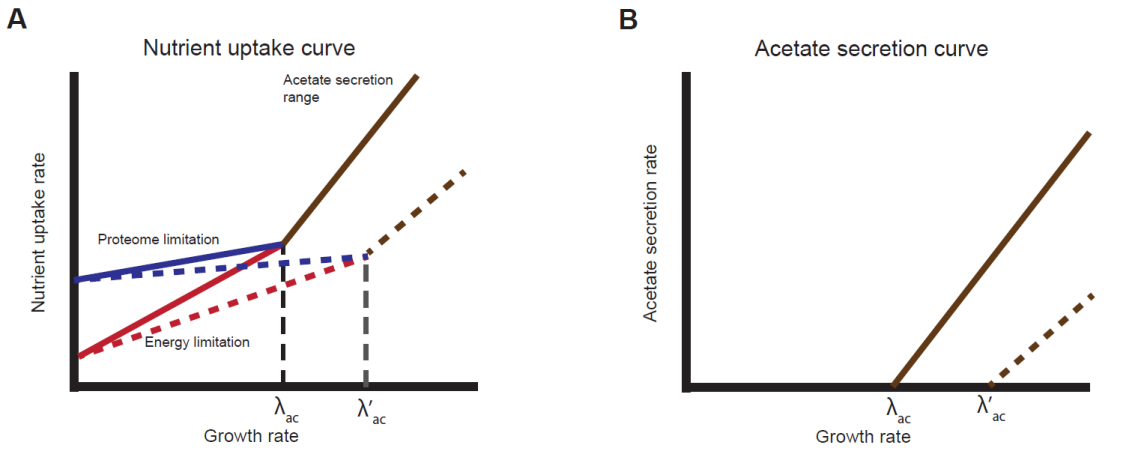

Figure 3 – Model solutions for growth with and without supplementation of a non-degradable biomass precursor. (A-B) Model predictions for the nutrient uptake rate (A) and acetate secretion rate (B) as function of growth rate. Solid lines depict model predictions for growth on a single nutrient source. Dashed lines depict model predictions for the effect of a non-degradable biomass precursor. Brown curves show model predictions for growth rates higher than the onset of acetate secretion; blue and red curves show model solutions for the proteome and energy-limited solutions respectively.

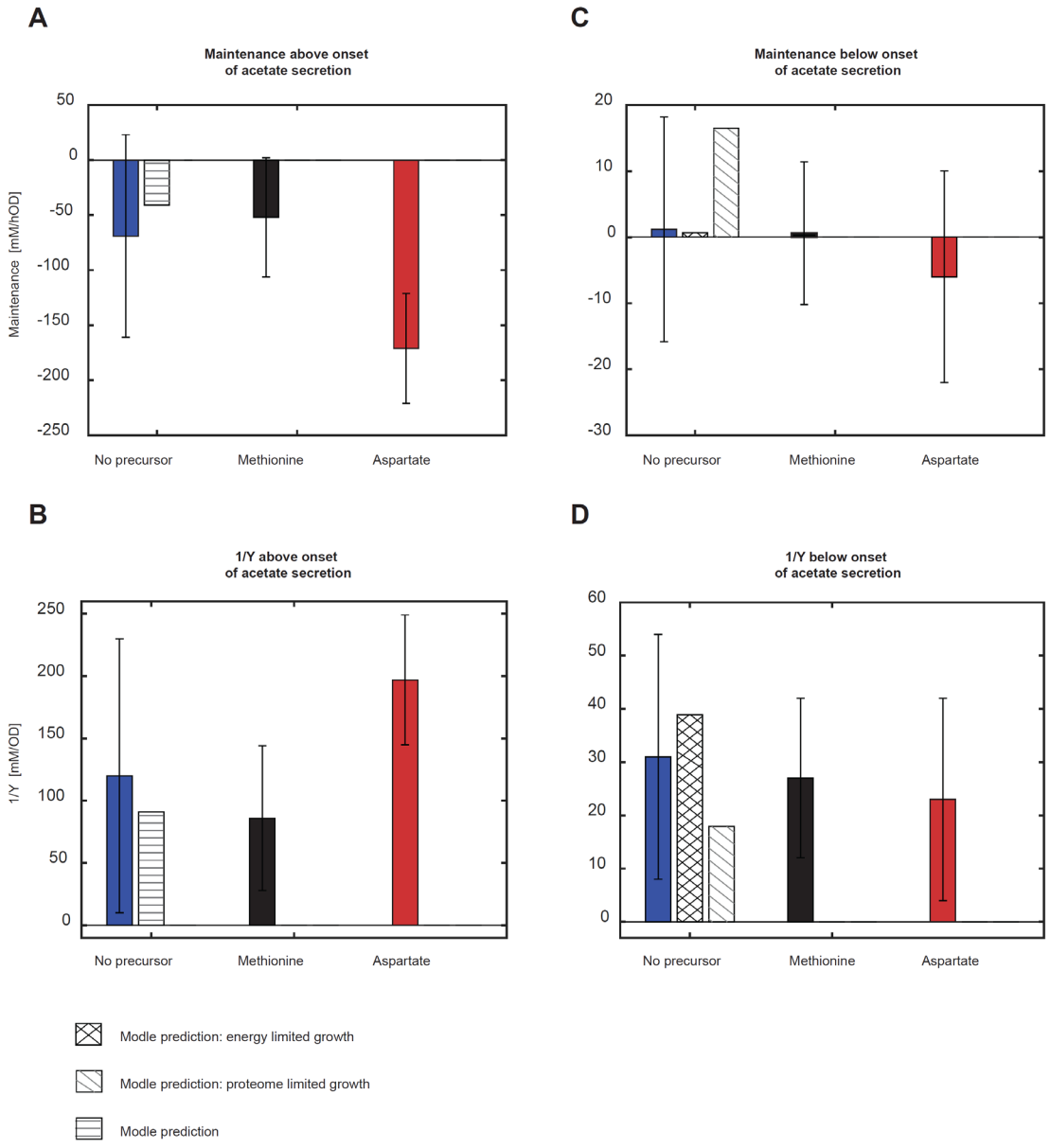

Figure 4 – Comparison of experimental results to model predictions. Comparison of the maintenance and reciprocal of the yield experimental results (solid bars) for growth on glucose or glucose with supplementation of methionine or aspartate compared to model predictions (dashed bars). **(A-B)** Growth rates above the onset of acetate secretion. **(C-D)** Growth rates below the onset of acetate secretion.

References

1. Pirt SJ. The maintenance energy of bacteria in growing cultures. Proc R Soc Lond B Biol Sci. 1965;163: 224–231.
2. Dawes EA, Ribbons DW. Some aspects of the endogenous metabolism of bacteria. Bacteriol Rev. 1964;28: 126–149.
3. Wallace RJ, Holms WH. Maintenance coefficients and rates of turnover of cell material in Escherichia coli ML308 at different growth temperatures. FEMS Microbiol Lett. 1986;37: 317–320.
4. Zeng H, Yang A. Bridging substrate intake kinetics and bacterial growth phenotypes with flux balance analysis incorporating proteome allocation. Sci Rep. 2020;10: 4283.
5. Neijssel OM, Tempest DW. Bioenergetic aspects of aerobic growth of Klebsiella aerogenes NCTC 418 in carbon-limited and carbon-sufficient chemostat culture. Arch Microbiol. 1976;107: 215–221.
6. Stouthamer AH, Bettenhaussen CW. Determination of the efficiency of oxidative phosphorylation in continuous cultures of Aerobacter aerogenes. Arch Microbiol. 1975;102: 187–192.
7. Pirt SJ. Maintenance energy: a general model for energy-limited and energy-sufficient growth. Arch Microbiol. 1982;133: 300–302.
8. Beyeler W, Rogers PL, Fiechter A. A simple technique for the direct determination of maintenance energy coefficient: an example with Zymomonas mobilis. Appl Microbiol Biotechnol. 1984;19: 277–280.
9. Tempest DW, Neijssel OM. The status of YATP and maintenance energy as biologically interpretable phenomena. Annu Rev Microbiol. 1984;38: 459–513.
10. Van Bodegom P. Microbial maintenance: a critical review on its quantification. Microb Ecol. 2007;53: 513–523.
11. Wang G, Post WM. A theoretical reassessment of microbial maintenance and implications for microbial ecology modeling. FEMS Microbiol Ecol. 2012;81: 610–617.
12. Russell JB, Cook GM. Energetics of bacterial growth: balance of anabolic and catabolic reactions. Microbiol Rev. 1995;59: 48–62.
13. Stouthamer AH, Bulthuis BA, Van Verseveld HW, Bazin MJ, Poole MJ, Keevil RK. Energetics of growth at low growth rates and its relevance for the maintenance concept. Microbial growth dynamics. 1990;28: 85–102.
14. Marr AG, Nilson EH, Clark DJ. The maintenance requirement of Escherichia coli. Ann N Y Acad Sci. 1963;102: 536–548.
15. Basan M. Resource allocation and metabolism: the search for governing principles. Curr Opin Microbiol. 2018;45: 77–83.
16. Zeng H, Rohani R, Huang WE, Yang A. Understanding and mathematical modelling of cellular resource allocation in microorganisms: a comparative synthesis. BMC Bioinformatics. 2021;22: 467. doi:10.1186/s12859-021-04382-3
17. Schulze KL, Lipe RS. Relationship between substrate concentration, growth rate, and respiration rate of Escherichia coli in continuous culture. Arch Mikrobiol. 1964;48: 1–20.

18. Chesbro W. The domains of slow bacterial growth. Can J Microbiol. 1988;34: 427–435.

19. Panikov NS. Microbial growth kinetics. 1995.

20. Russell JB, Cook GM. Energetics of bacterial growth: balance of anabolic and catabolic reactions. Microbiol Rev. 1995;59: 48–62.

21. Grigaitis P, Grundel DAJ, van Pelt-KleinJan E, Isaku M, Xie G, Mendoza Farias S, et al. A computational toolbox to investigate the metabolic potential and resource allocation in fission yeast. mSystems. 2022;7: e00423-22.

22. Conway T. Aspartate in the intestine: dual service as anaerobic electron acceptor and nitrogen source. Environ Microbiol. 2021;23: 2364–2365.

23. Schubert C, Winter M, Ebert-Jung A, Kierszniowska S, Nagel-Wolfrum K, Schramm T, et al. C4-dicarboxylates and l-aspartate utilization by Escherichia coli K-12 in the mouse intestine: l-aspartate as a major substrate for fumarate respiration and as a nitrogen source. Environ Microbiol. 2021;23: 2564–2577.

24. Basan M, Hui S, Okano H, Zhang Z, Shen Y, Williamson JR, et al. Overflow metabolism in Escherichia coli results from efficient proteome allocation. Nature. 2015;528: 99–104. doi:10.1038/nature15765

25. Hui S, Silverman JM, Chen SS, Erickson DW, Basan M, Wang J, et al. Quantitative proteomic analysis reveals a simple strategy of global resource allocation in bacteria. Mol Syst Biol. 2015;11: 784.

26. Scott M, Gunderson CW, Mateescu EM, Zhang Z, Hwa T. Interdependence of cell growth and gene expression: origins and consequences. Science. 2010;330: 1099–1102.

27. You C, Okano H, Hui S, Zhang Z, Kim M, Gunderson CW, et al. Coordination of bacterial proteome with metabolism by cyclic AMP signalling. Nature. 2013;500: 301–306.

28. Varma A, Palsson BO. Metabolic flux balancing: basic concepts, scientific and practical use. Bio/technology. 1994;12: 994–998.

29. Neidhardt FC, Ingraham JL, Schaechter M. Physiology of the bacterial cell. Sinauer associates; 1990.

30. Nelson DL, Lehninger AL, Cox MM. Lehninger principles of biochemistry. Macmillan; 2008.

31. Peebo K, Valgepea K, Maser A, Nahku R, Adamberg K, Vilu R. Proteome reallocation in Escherichia coli with increasing specific growth rate. Mol Biosyst. 2015;11: 1184–1193.

32. O'brien EJ, Lerman JA, Chang RL, Hyduke DR, Palsson BØ. Genome-scale models of metabolism and gene expression extend and refine growth phenotype prediction. Mol Syst Biol. 2013;9: 693.

33. Molenaar D, Van Berlo R, De Ridder D, Teusink B. Shifts in growth strategies reflect tradeoffs in cellular economics. Mol Syst Biol. 2009;5: 323.

34. Mori M, Hwa T, Martin OC, De Martino A, Marinari E. Constrained allocation flux balance analysis. PLoS Comput Biol. 2016;12: e1004913.

35. Goelzer A, Fromion V. Bacterial growth rate reflects a bottleneck in resource allocation. Biochimica et Biophysica Acta (BBA)-General Subjects. 2011;1810: 978–988.

36. Varma A, Boesch BW, Palsson BO. Stoichiometric interpretation of Escherichia coli glucose catabolism under various oxygenation rates. Appl Environ Microbiol. 1993;59: 2465–2473.

37. O'brien EJ, Lerman JA, Chang RL, Hyduke DR, Palsson BØ. Genome-scale models of metabolism and gene expression extend and refine growth phenotype prediction. Mol Syst Biol. 2013;9: 693.

38. Lerman JA, Hyduke DR, Latif H, Portnoy VA, Lewis NE, Orth JD, et al. In silico method for modelling metabolism and gene product expression at genome scale. Nat Commun. 2012;3: 929.

39. Nilsson A, Nielsen J, Palsson BO. Metabolic models of protein allocation call for the kinetome. Cell Syst. 2017;5: 538–541.

40. Zinn M, Witholt B, Egli T. Dual nutrient limited growth: models, experimental observations, and applications. J Biotechnol. 2004;113: 263–279.

41. Lendenmann U, Egli T. Kinetic models for the growth of Escherichia coli with mixtures of sugars under carbon-limited conditions. Biotechnol Bioeng. 1998;59: 99–107.

42. Egli T. On multiple-nutrient-limited growth of microorganisms, with special reference to dual limitation by carbon and nitrogen substrates. Antonie Van Leeuwenhoek. 1991;60: 225–234.

43. Wang X, Xia K, Yang X, Tang C. Growth strategy of microbes on mixed carbon sources. Nat Commun. 2019;10: 1279. doi:10.1038/s41467-019-09261-3

44. Zamboni N, Mouncey N, Hohmann H-P, Sauer U. Reducing maintenance metabolism by metabolic engineering of respiration improves riboflavin production by Bacillus subtilis. Metab Eng. 2003;5: 49–55.

45. Li X-J, Chen T, Chen X, Zhao X-M. Redirection electron flow to high coupling efficiency of terminal oxidase to enhance riboflavin biosynthesis. Appl Microbiol Biotechnol. 2006;73: 374–383. doi:10.1007/s00253-006-0482-7

46. Gommers PJF, Van Schie BJ, Van Dijken JP, Kuenen JG. Biochemical limits to microbial growth yields: an analysis of mixed substrate utilization. Biotechnol Bioeng. 1988;32: 86–94.

47. Barton MD, Delneri D, Oliver SG, Rattray M, Bergman CM. Evolutionary systems biology of amino acid biosynthetic cost in yeast. PLoS One. 2010;5: e11935.

48. Kaleta C, Schäuble S, Rinas U, Schuster S. Metabolic costs of amino acid and protein production in Escherichia coli. Biotechnol J. 2013;8: 1105–1114. doi:10.1002/biot.201200267

49. Akashi H, Gojobori T. Metabolic efficiency and amino acid composition in the proteomes of Escherichia coli and Bacillus subtilis. Proc Natl Acad Sci U S A. 2002;99: 3695–3700. doi:10.1073/pnas.062526999

50. Zhang H, Wang Y, Li J, Chen H, He X, Zhang H, et al. Biosynthetic energy cost for amino acids decreases in cancer evolution. Nat Commun. 2018;9: 4124.

51. Swire J. Selection on Synthesis Cost Affects Interprotein Amino Acid Usage in All Three Domains of Life. J Mol Evol. 2007;64: 558–571. doi:10.1007/s00239-006-0206-8

52. Seligmann H. Cost-minimization of amino acid usage. J Mol Evol. 2003;56: 151–161.

53. Heizer Jr EM, Raiford DW, Raymer ML, Doom TE, Miller R V, Krane DE. Amino acid cost and codon-usage biases in 6 prokaryotic genomes: a whole-genome analysis. Mol Biol Evol. 2006;23: 1670–1680.

54. Chen Y, Nielsen J. Yeast has evolved to minimize protein resource cost for synthesizing amino acids. Proceedings of the National Academy of Sciences. 2022;119: e2114622119.

55. Wagner A. Energy constraints on the evolution of gene expression. Mol Biol Evol. 2005;22: 1365–1374.

56. Raiford DW, Heizer EM, Miller R V, Akashi H, Raymer ML, Krane DE. Do amino acid biosynthetic costs constrain protein evolution in Saccharomyces cerevisiae? J Mol Evol. 2008;67: 621–630.

57. Zampieri M, Hörl M, Hotz F, Müller NF, Sauer U. Regulatory mechanisms underlying coordination of amino acid and glucose catabolism in Escherichia coli. Nat Commun. 2019;10: 3354.

58. Golan O, Gampp O, Eckert L, Sauer U. Overall biomass yield on multiple nutrient sources. bioRxiv. 2023; 2023.02.16.528813. doi:10.1101/2023.02.16.528813

59. McGuffee SR, Elcock AH. Diffusion, crowding & protein stability in a dynamic molecular model of the bacterial cytoplasm. PLoS Comput Biol. 2010;6: e1000694.

60. Höfling F, Franosch T. Anomalous transport in the crowded world of biological cells. Reports on Progress in Physics. 2013;76: 046602.

61. Klumpp S, Scott M, Pedersen S, Hwa T. Molecular crowding limits translation and cell growth. Proceedings of the National Academy of Sciences. 2013;110: 16754–16759.

62. Javanainen M, Hammaren H, Monticelli L, Jeon J-H, Miettinen MS, Martinez-Seara H, et al. Anomalous and normal diffusion of proteins and lipids in crowded lipid membranes. Faraday Discuss. 2013;161: 397–417.

63. Dix JA, Verkman AS. Crowding effects on diffusion in solutions and cells. Annu Rev Biophys. 2008;37: 247–263.

64. Biselli E, Schink SJ, Gerland U. Slower growth of Escherichia coli leads to longer survival in carbon starvation due to a decrease in the maintenance rate. Mol Syst Biol. 2020;16: e9478.

65. Schink SJ, Biselli E, Ammar C, Gerland U. Death Rate of E. coli during Starvation Is Set by Maintenance Cost and Biomass Recycling. Cell Syst. 2019;9: 64-73.e3. doi:https://doi.org/10.1016/j.cels.2019.06.003

66. Anderson T-H, Domsch KH. Determination of ecophysiological maintenance carbon requirements of soil microorganisms in a dormant state. Biol Fertil Soils. 1985;1: 81–89.

67. Krömer JO, Wittmann C, Schröder H, Heinzle E. Metabolic pathway analysis for rational design of L-methionine production by Escherichia coli and Corynebacterium glutamicum. Metab Eng. 2006;8: 353–369.

68. Ykema A, Bakels RHA, Verwoert IIGS, Smit H, van Verseveld HW. Growth yield, maintenance requirements, and lipid formation in the oleaginous yeast Apiotrichum curvatum. Biotechnol Bioeng. 1989;34: 1268–1276.

69. Abbott BJ, Clamen A. The relationship of substrate, growth rate, and maintenance coefficient to single cell protein production. Biotechnol Bioeng. 1973;15: 117–127.

70. Bevington PR, Robinson DK, Blair JM, Mallinckrodt AJ, McKay S. Data reduction and error analysis for the physical sciences. Computers in Physics. 1993;7: 415–416.

Chapter 3 – Overall biomass yield on multiple nutrient sources

Ohad Golan[1, 2], Olivia Gampp[1], Lina Eckert[1], Uwe Sauer[1*]

[1] Institute of Molecular Systems Biology, ETH Zürich, Otto-Stern-Weg 3, 8093 Zürich, Switzerland

[2] Life Science Zurich PhD Program on Systems Biology, Zurich, Switzerland

Author contributions

OGo conceived and designed the study, designed experiments, performed experiments, analyzed data and wrote the manuscript. OGa performed experiments. LE designed experiments. US wrote the manuscript.

Abstract

Microorganisms utilize nutrients primarily to generate biomass and replicate. When a single nutrient source is available, the produced biomass increases linearly with the initial amount of the available nutrient. This linear trend can be predicted to high accuracy by "black box models" that consider growth as a single chemical reaction with nutrients as substrates and biomass as a product. Since natural environments typically feature multiple nutrients, we extended the black box framework to include catabolism, anabolism, and biosynthesis of biomass precursors to quantify co-utilization of multiple nutrients on microbial biomass production. The model differentiates between different types of nutrients: degradable nutrients that first must be catabolized before they can be used from non-degradable nutrients that can only be used as a biomass precursor. Experimentally, we demonstrated that contradictory to the model predictions, there is a mutual effect between different nutrients on *Escherichia coli's* nutrient utilization, where the ability to utilize one is affected by the other; i.e., for some combinations the produced biomass was no longer linear to the initial amount of nutrients. To capture such mutual effects with a black box model, we phenomenologically added an interaction between the metabolic processes used in utilizing the nutrient sources. The phenomenological model qualitatively captures the experimental observations and, unexpectedly, predicts that the produced biomass does not only depend on the combination of nutrient sources but also on their relative initial amounts – a prediction we validated experimentally. Moreover, the model predicts which metabolic processes – catabolism, anabolism, or precursor biosynthesis – is affected in each nutrient combination.

Introduction

Natural environments are characterized by a broad spectrum of physicochemical parameters that collectively define constraints within which species survive and thrive. Of particular importance to niche occupancy by different microbes are the type of nutrients and their temporal availability. For example, bacteria growing in a riverbed might experience continuous nutrient flux and high spatial homogeneity while bacteria growing in pulsating

environments, such as tidal wetlands or at the sea bottom, receive nutrients only sporadically [1,2]. Different physiological traits provide fitness advantages for different nutrient dynamics. Continuous nutrient flux environments favor organisms with higher growth rate so that they can exploit the otherwise washed out nutrients, while environments of sporadic nutrient flux and high spatial heterogeneity favor organisms that utilize resources more efficiently [3–6].

In conditions of continuous nutrient flux, the biomass produced per consumed nutrient is physiologically defined as the biomass yield parameter that describes the efficiency of nutrient utilization [7–9]. Theoretical models, known as 'black box models', predict the biomass yield for growth on a single nutrient source in conditions of continuous flux such as those observed in chemostat experiments to high accuracy [10–12]. These models consider growth as a single chemical reaction with the nutrients as substrates and the produced biomass and secreted byproducts as products. By calculating the change in free energy of the whole reaction, the biomass yield is predicted. Here, we adopt these models to qualitatively predict and then test the overall biomass yield in batch cultures of *Escherichia coli*, where the outgoing flux of nutrients is limited so that all available nutrients is utilized, including reutilization of secreted byproducts, a condition akin to a single nutrient pulse in natural pulsating environments. Since natural environments typically contain multiple nutrients [13–15], we investigate whether the overall biomass yield of a nutrient depends on the availability and metabolic properties of a second nutrient, for example if it can be degraded or only used as a building block for biomass.

Generally, black box models describe scenarios without mutual effects between nutrients; hence, the overall biomass yield of each nutrient is independent of the availability of another. We tested this prediction experimentally by titrating a second nutrient to batch cultures grown on a single carbon source, demonstrating that the overall biomass yield depends not only on the availability but also on the initial amount of other nutrients, and that this mutual effect can be negative. To explain these observations, we expanded the black box model to consider whether a second nutrient can only be used for biomass synthesis or also degraded for energy generation and included mutual effects between the metabolic processes of the nutrient

sources. The model qualitatively captures the experimental observations and explains how the combination of nutrients affects metabolism. Furthermore, using the model, we determine the mutual effect of different nutrient combinations on growth processes.

Results

Growth on a single nutrient source

The classical system to investigate the efficiency of nutrient utilization in pulsating environments where organisms have sufficient time to fully utilize all available nutrients in a single nutrient pulse are batch cultures. Here we follow growth of *E. coli* until depletion of the initial nutrient source and potential secreted byproducts when stationary phase is reached in M9 minimal medium with glucose, malate, or aspartate as sole carbon sources [16,17]. These carbon sources were chosen as respiro-fermentative, strictly respiratory, and a degradable biomass component. The produced biomass (ΔB), that is the biomass reached at stationary phase minus the biomass at inoculation, was recorded as the optical density at 600nm, converted to cellular dry weight using a predetermined conversion factor [18], and plotted against the initial nutrient amount (Fig 1; S1 Fig). The produced biomass shows a good linear fit to the initial amount of the sole carbon source (Fig 1B) and as such, can be described by [16]:

(1) $\Delta B = Y_{X/D} N_D$

where N_D is the initial amount of nutrient D and $Y_{X/D}$ the overall biomass yield for organism X on nutrient D which describes the efficiency of full utilization of the available nutrient.

Fig 1. Overall biomass yield of malate (A) Growth curves of *E. coli* for different initial amounts of malate. Curves are averages of three biological replicates. The produced biomass (ΔBM) is the final biomass reached in stationary phase minus the initial biomass at inoculation. (B) The produced biomass of the different growth curves in Fig 1A as function of the initial nutrient amount. The slope of the linear fit is the overall biomass yield (fit parameter R^2>0.9).

Bars of standard errors of the biological replicates are too small to be noticeable. Data for glucose and aspartate experiments are shown in S1 Fig.

To predict the produced biomass, we used a black box formalism [10] that separates the growth reaction of chemotrophic organisms to a two-reaction process (Fig 2A). The first is a catabolic reaction that releases Gibbs free energy by breakdown of nutrients. The second is the anabolic reaction that uses the released free energy for the synthesis of new biomass. The overall Gibbs energy dissipation ΔG_X of the growth process is given by ([10], S1A text):

(2) $\Delta G_X = \frac{1}{Y_{X/D}} \Delta G_{cat} + \Delta G_{an}$

where the subscripts *cat,* and *an* refer to the Gibbs energy of dissipation of the catabolic and anabolic reactions, respectively. Given that all secreted byproducts are utilized in the here investigated growth conditions, the free energy of the secreted byproducts can be set to 0, the overall biomass yield may be predicted as [10]:

(3) $Y_{X/D} = \frac{\Delta G_{cat}}{\Delta G_X - \Delta G_{an}}$

Combining equations (1) and (3) predicts a linear correlation of the produced biomass as function of initial nutrient amount with a slope that depends only on the type of nutrient through ΔG_{cat}. This prediction fits qualitatively well with all measured nutrients [16,17] (Fig 1B, S1 Fig).

Growth on multiple nutrient sources

Since organisms typically encounter multiple nutrients in natural environments, we next asked whether the availability of one nutrient affects the overall biomass yield of another. To enable a black box model to capture such effects, we added another reaction that depends on the type of second nutrient: A) degradable nutrients that first must be catabolized before they can be used, such as a sugar; B) non-degradable nutrients that can be used only as a biomass precursor, such as the non-degradable amino acid methionine in *E. coli*; and C) nutrients that can be both catabolized or used directly as a biomass precursor, such as the amino acid

aspartate in *E. coli*. For the combination of two degradable nutrients the added reaction is catabolic (S1B text, Fig 2B). In this case, the overall Gibbs energy dissipation gives:

(4) $\Delta G_X = \frac{1}{Y_{X/N_1}} \Delta G_{cat}^{N_1} + \frac{1}{Y_{X/N_2}} \Delta G_{cat}^{N_2} + \Delta G_{an}$

where $\Delta G_{cat}^{N_i}$ is the Gibbs energy of dissipation for the catabolic process of nutrient i. When the second nutrient source is a non-degradable biomass precursor, we split the anabolic reaction into two – a reaction for biosynthesis of the biomass precursor and a reaction for the general anabolic process (S1C text, Fig 2C). The overall Gibbs energy of dissipation in this case gives:

(5) $\Delta G_X = \frac{1}{Y_{X/N_1}} \Delta G_{cat} + \Delta G_{an}^{bsyn} + \Delta G_{bsyn}(1 - M_{utl})$

where ΔG_{bsyn} is the Gibbs energy of dissipation for synthesis of the biomass precursor and ΔG_{an}^{bsyn} is the dissipation energy for the general anabolic process minus that of the biomass precursor. The function M_{utl} describes the ratio of available biomass precursor to that required to generate the produced biomass during the growth process. It is dependent on biomass precursor availability such that when all the necessary biomass precursor is available in the environment, the function assumes the maximal value of 1 and the cost for this precursor biosynthesis is alleviated.

Combining equations (4) or (5) with equation (1) shows that regardless of the type of nutrient supplemented, the produced biomass is predicted to be a linear sum of the biomass gained from the available nutrients and the overall biomass yield of each nutrient is independent of the availability of others (S1B-C text, Fig 2D):

(6) $\Delta B = Y_{X/N1}\, N_1 + Y_{X/N2} N_2$

where N_i is the amount of nutrient i in the growth medium and $Y_{X/Ni}$ is the overall biomass yield of nutrient i.

To test the prediction that the overall biomass yield of a nutrient is independent of the availability of others, we compared the overall biomass yield of *E. coli* for different nutrients,

henceforth referred to as the measured nutrient, in the presence or absence of a second nutrient, termed the base nutrient. To do so, the initial amount of the measured nutrient was varied for each batch culture experiment at constant initial amounts of the base nutrient between 0 and 1.2 g/l for glucose, acetate, or aspartate and 0 and 0.06 g/l for methionine. The produced biomass was plotted against the initial amount of the measured nutrient and the overall biomass yield was determined as the slope of a linear fit of that curve (Fig 3A,B). In combination with glucose, succinate, or acetate as base nutrients, we determined the overall biomass yield of xylose and methionine as measured nutrients, as examples of degradable or non-degradable nutrients, respectively (Fig 3). The initial amount of base nutrient determines the intercept with the Y-axis and was chosen such that the measured parameters remain within measurable range.

The overall biomass yield was highly dependent on the base nutrient. For xylose, the overall biomass yield was higher on succinate as base nutrient than on glucose or when used alone, and for methionine the overall yield was by far the highest on glucose (Fig 3C,D). For most combinations, the influence of the second nutrient was monotonous across the tested concentrations, i.e., the overall biomass yield of the measured nutrient can be determined from the slope of a linear fit (Fig 3A,B). An exception was the non-monotonous behavior of methionine as the measured nutrient in combination with glucose as a base nutrient (Fig 3B). At low initial amounts of methionine (below 3 μg), increasing initial amounts of methionine unexpectedly decreased the produced biomass. In the higher range of initial amounts (above 3 μg), increasing methionine initial amounts increased the produced biomass linearly.

Thus, the overall biomass yield of a measured nutrient is dependent on the base nutrient, consequently black box theory cannot capture the produced biomass of multiple nutrient sources. To enable the model to describe such mutual effects, we expand it to include such effects phenomenologically. To do so, we coupled a function that is dependent on the combination of available nutrients to the Gibbs energy dissipation of each reaction in the

growth processes. For simplicity, we assumed these functions are linear to the initial nutrient amount.

As such, the overall Gibbs energy dissipation of growth on two degradable nutrient sources is described as (S1D text):

(7) $\Delta G_X = \frac{1}{Y_{X/N_1}} \Delta G_{cat}^{N_1} f_{cat1}(N_2) + \frac{1}{Y_{X/N_2}} \Delta G_{cat}^{N_2} f_{cat2}(N_1) + \Delta G_{an} f_{an}(N_1, N_2)$

where $f_{cat}(N_i)$, $f_{an}(N_i)$ are linear functions to the initial amounts of nutrient source i, with coefficients $\mathrm{m}_{\mathrm{cat}}^{\mathrm{N_j}}$, $\mathrm{m}_{\mathrm{an}}^{\mathrm{N_j}}$ respectively. These functions phenomenologically depict the mutual effect of the nutrient combination on the growth processes. Combining equations (1) and (7) predicts the produced biomass:

(8) $\Delta B = \frac{\Delta G_{cat}^{N_1} N_1 + \Delta G_{cat}^{N_2} N_2 + \Delta \mathrm{m}_{\mathrm{CAT}}^{\mathrm{N_1 N_2}} N_1 N_2}{\Delta G_X - \Delta G_{an} f_{an}(N_1, N_2)}$

where $\Delta \mathrm{m}_{\mathrm{CAT}}^{\mathrm{N_1 N_2}} = \Delta G_{cat}^{N_1} m_{cat}^{N_1} + \Delta G_{cat}^{N_2} m_{cat}^{N_2}$ and $f_{an}(N_1, N_2) = 1 + m_{an}^{N_1} N_1 + m_{an}^{N_2} N_2$. Given a mutual effect between nutrients, the produced biomass is thus made of three terms, two describing the direct effect of catabolism of the two nutrient sources and a third term describing the mutual catabolic effect depending on availability of both substrates. Exploring the solution space of the model shows that, depending on the type of mutualism, qualitatively different relationships are predicted between available nutrients and biomass formation (Fig 4A) – a positive mutual catabolic effect increases the overall biomass yield (Fig 4A, orange curve) while a negative catabolic effect decreases it (Fig 4A, purple curve). The expanded model can capture the experimentally observed mutual effect of increased overall biomass yield with a positive mutual catabolic effect (compare increased slope for different base nutrients in Fig 3A to the orange curve in Fig 4A).

For growth on a combination of a degradable nutrient and a non-degradable biomass precursor, the overall Gibbs energy dissipation is described as (S1E text):

(9) $\Delta G_X = \frac{1}{Y_{X/D}} \Delta G_{cat} f_{cat}(M) + \Delta G_{an} f_{an}(N, M) + \Delta G_{bsyn}^{M} f_{bsyn}(N)(1 - M_{utl})$

where $f_{cat}(M_{utl})$, $f_{an}(N, M_{utl})$, $f_{bsyn}(M_{utl})$ are linear functions with coefficients m_{cat}, m_{an}^{N}, m_{an}^{M}, m_{sbyn} respectively. These functions depict the mutual effect between the nutrient sources on the Gibbs free energy of each growth reaction. Solving equations (1) and (9) for the produced biomass gives a quadratic equation:

$$\Delta B^2 - \frac{\Delta B}{\Delta G_A}\left(N\Delta G_{cat} + M'\left(m_{an}^{M}\,\Delta G_{an} - \left(1 + m_{sbyn}N\right)\Delta G_{bsyn}^{M}\right)\right) - N\frac{\Delta G_{cat}}{\Delta G_A}m_{cat}M' = 0 \quad (10)$$

where $\Delta G_A = \left(\Delta G_X - \Delta G_{an}(1 - Nm_{an}^{N}) - \Delta G_{bsyn}^{M}\left(1 + m_{sbyn}N\right)\right)$ and $M' = M_{utl}\Delta B$.

Unlike the solution for growth on two degradable nutrient sources, solving equation (10) for the produced biomass shows that a mutual effect between a biomass precursor and a degradable nutrient can give rise to non-monotonous solutions. Fig 4B explores the solution space of possible mutual effects between a precursor and a degradable nutrient. The case of a negative catabolic effect (Fig 4B, orange curve) fits qualitatively well with the experimental observation of the biomass precursor methionine on glucose as base nutrient (Fig 3B, green data points).

The coefficients of the linear functions depicting the mutual effect between the nutrients are a key output of the model since they infer how each combination of nutrients effects the different growth reactions. Fitting these coefficients to the experimental results of methionine growing with glucose as a base nutrient gives a qualitative fit to a negative value for the catabolic parameter (coefficient m_{cat}), revealing that methionine decreases the catabolic efficiency of glucose. Furthermore, the overall biomass yield of methionine on glucose in the linear region is higher than that on succinate or acetate (Fig 3D), suggesting a mutual effect on another metabolic process in one of these combinations, potentially the precursor biosynthesis processes (coefficient m_{sbyn}). For all combinations of two degradable nutrients, the overall biomass yield increased as compared to growth on sole nutrient sources (Fig 3C), a result that fits a positive mutual effect on the catabolic process (coefficient m_{cat}).

An unexpected model prediction is noticeable in equations (9) and (10) where the initial amounts of the two available nutrients are coupled in at least one term. Hence, the model predicts that the overall biomass yield of a measured nutrient depends not only on the

availability of a base nutrient, but also on the relative initial amounts of the nutrients. For a combination of two degradable nutrient sources with a positive catabolic effect, as observed experimentally for xylose on the two base nutrients (Fig 3A,C), the overall biomass yield is predicted to increase with increasing initial amounts of the base nutrient (Fig 4C). For the combination of a degradable nutrient and a biomass precursor, such as methionine on glucose, with a negative catabolic effect and positive effect on precursor biosynthesis, the model predicts a shift of the curves for the non-linear part as well as an increase in the slope of the linear part with increasing initial amounts of base nutrient (Fig 4D).

To test these predictions, we determined the produced biomass on xylose and methionine as the measured nutrients on different initial amounts of succinate and glucose as the base nutrients, respectively (Fig 5A,B). The overall biomass yield of xylose (i.e., slope of the curve) increased linearly with the initial amount of the base nutrient succinate (Fig 5A, C). This observation fits well with the model prediction for a positive catabolic effect between two degradable nutrients (Fig 4C). The curve of the produced biomass on methionine exhibits a more complex dependency on the initial amount of glucose as the base nutrient. Above $5\ \mu g$ methionine, the slope of all curves increased linearly with the amount of the base nutrient glucose, but below $5\ \mu g$ methionine there was no linear dependency and the amount of base nutrient varied the curve shape (Fig 5B, D). This observation fits well with the theoretical prediction (Fig 4D) that this nutrient combination not only has a positive effect on the precursor biosynthesis reaction (i.e., the linear dependency at higher methionine supplementation), but also a negative catabolic effect where at low methionine concentrations, in some cases, more methionine leads to lower biomass gain.

Which mechanism underlies the negative catabolic effect of methionine on glucose? The growth curves followed the classical diauxic shift with exponential growth on glucose and a second phase on previously secreted acetate (S2A Fig). For the example of 160 μg glucose as the base nutrient (Fig 5, pink curve), the first phase lasted 4-4.5 hours and growth on acetate resumed between 7-10 hours (S2A Fig). In both phases, the biomass gain (calculated as the

biomass at the end minus the biomass at the beginning) increased linearly with methionine amounts greater than 2 μg (S2B, C Fig). The biomass gain was much higher than the trendline in the absence of or at very low methionine concentrations. During exponential growth on glucose in the first phase, methionine decreased the gain in biomass but increased the growth rate (S2D Fig.). Given the diauxic shift from growth on glucose to previously secreted acetate (S2E Fig), the most plausible explanation for the higher biomass gain without or low methionine in the second phase is due to higher acetate secretion in the first phase. To test whether methionine supplementation indeed reduced acetate secretion, we varied acetate secretion rates by altering steady state growth through an inducible promoter for the glucose uptake gene *ptsG* that limits glucose uptake [19]. Comparing acetate secretion in the presence and absence of methionine shows that methionine indeed decreases acetate secretion (S2F Fig). Thus, the negative catabolic effect of methionine on glucose catabolism appears to be a combination of a lower biomass gain during the first growth phase, with a higher growth rate and less acetate secretion, and a lower biomass gain in the second phase because less acetate was secreted.

At the lowest amounts of methionine (0 and 1.43 μg) we noted a shorter lag time for growth on acetate (S2A Fig, compare red and black curves to the other curves). Growth with 1.43 μg methionine was somewhat special as it followed the biomass trendline in the first growth phase but could not sustain the higher growth rate throughout this growth phase (S2A Fig, red curve between 2-4h), presumably because methionine was used up, which explains why its biomass gain in the second phase was indistinguishable from the no methionine condition (S2C Fig). Consistently, 1.43 μg methionine was below the amount necessary to produce the biomass reached at the end of the first growth phase (about 1.7 μg of methionine is required to generate 0.8 gDCW of biomass [20]).

Growth with a second nutrient that can be degraded and used as a biomass precursor

So far, we focused on degradable nutrients or nutrients that can only be used as biomass precursors. Some nutrients such as degradable amino acids, however, can be directly used

both as biomass precursors or energy source. Given the complex curves observed for the combination of biomass precursor and degradable nutrient, we expected that a degradable amino acid in combination with a degradable nutrient would also produce non-monotonous curves. To investigate the effects of such nutrient combinations, we measured the produced biomass on the degradable amino acid aspartate on different initial amounts of glucose and acetate as base nutrients (Fig 6A,B). The combination of aspartate and acetate led to a complex curve with two linear phases separated by a double shift in slope at intermediate concentrations (between $100 - 150\ \mu g$, Fig 6A). The first phase at low initial amounts of aspartate resulted in a linear slope that increases with initial amount of acetate while the slope of the second phase shows only a low dependency on acetate initial amounts (Fig 6C). Aspartate on glucose also shows a complex curve with two linear phases (Fig 6B). In this nutrient combination, the slope of the first phase is independent of the initial amount of glucose yet the length of this phase increases with increasing initial glucose amounts (Fig 6D). The slope of the second linear phase increases with increasing glucose initial amounts. The complex behavior observed in these experiments cannot be captured even with the mutual effect model presented here. We hypothesize that the ratio of how much aspartate is utilized as a biomass precursor to how much is catabolized affects the overall biomass yield. The multiple utilization possibilities add an additional degree of freedom to the system and as such, capturing the behavior of these nutrients in a model requires time-resolved intracellular flux information.

Discussion

In conditions of low nutrient flux, organisms utilize all nutrients in the environment and reabsorb previously secreted byproducts to fuel further growth. Here we asked whether the availability of one nutrient affects the utilization efficiency of another? We showed that different nutrient combinations have different mutual effects on an organism's ability to generate biomass, presumably by changing intracellular metabolism, secretion, and reabsorption of secreted byproducts. While microbial utilization of multiple nutrients has been extensively

studied, yielding significant findings like the diauxic shift [21–23] or the complex interplay of factors in multiple nutrient environments [24–27], these studies don't differentiate between different nutrient types, focus on specific growth phases and as such are incapable of capturing the biomass gain from the entire growth curve.

To address this challenge and gain a more comprehensive understanding, we expanded previous black box models to depict the full growth process for growth on multiple nutrients. We expanded the model to account for the effect of different nutrient types and incorporated a phenomenological representation of mutual effects between nutrient sources. The expanded black box model was able to qualitatively capture the experimental observation and further predicts that the overall biomass yield of a nutrient depends not only on the availability of other nutrients but also on the ratio of initial amounts of the different nutrients. Given the coarse granularity of a black box model, it does not identify the specific metabolic reactions. However, by fitting the model to experimental measurements, the model can determine which coarse-grained metabolic process – catabolism, anabolism or precursor biosynthesis – in each nutrient combination is the cause of the mutual effect. This leads to generate hypotheses on which specific pathways are affected. For instance, we observed that for *E. coli* growing on glucose, methionine supplementation decreases the catabolic efficiency of glucose utilization, and provide circumstantial evidence that this is caused by a combination of the effect of methionine on the growth rate and reduced acetate secretion.

For all nutrient combinations, the initial amount of the base nutrient had a positive effect on the overall biomass yield of the measured nutrient, for at least some region of the measured range. This result is consistent with previous reports, for example, the supplementation of growth media with casamino acids or yeast extract has been shown to increase the carbon utilization efficiency of succinate or asparagine in batch culture experiments of *Enterobacter aerogenes* and *Pseudomonas perfectomarinus* [28]. Similarly, the utilization of mixtures of different dissolved organic carbon sources by bacterial communities in aquatic systems has been found to be more efficient than the utilization of a single source [29–33]. Moreover, the carbon

utilization efficiency of *Candida utilis*, *P. oxalaticus*, *Saccharomyces cerevisiae*, *Paracoccus denitrificans*, and *Thiobacilius versutus* has been found to be higher than theoretically predicted when a nutrient source that can be utilized solely as an energy source was supplemented during balanced growth conditions [34–36]. It is tempting to conclude that the underlying reason for this deviation from the theoretical prediction is similar in all cases, regardless of the experimental setup and measured parameter, i.e., biomass yield as measured in a chemostat continuous culture [7–9] or the overall biomass yield as measured in batch cultures. Our analysis suggests that the different nutrients affect each other's catabolism, although the specific metabolic pathways that are affected remain unresolved. One potential explanation could lie in the concept of maintenance energy, which can potentially vary depending on nutrient availability. A maintenance energy that decreases due to supplementation of a second nutrient would consequently increase the efficiency of nutrient utilization. To further investigate these mechanisms and identify a possible global mechanism, a more detailed resolution of metabolic pathways and their fluxes will be necessary, possibly by combining the thermodynamic black-box approach presented here with genome-scale metabolic models [37,38].

Inherent to the black box models is the conception that the biomass produced is ultimately constrained by the energy available in the system. These models hinge on a thermodynamic balance, where the energy gleaned from catabolic processes is weighed against the energy expended in anabolic processes. While these models address the energy balance, implications for the carbon balance can extrapolated from the results. Given the conservation of carbon in the system, our findings suggest that the combination of nutrients could have a substantial impact on CO_2 production as the primary carbon byproduct during growth. In cases where a base nutrient augments the yield of the measured nutrient, CO_2 production per nutrient utilized would decrease, while a base nutrient that diminishes the yield of the measured nutrient can result in an increase in CO_2 production per nutrient utilized.

Understanding the influence of nutrient combinations on CO_2 production opens up broader ecological considerations, especially when changes in CO_2 production can significantly impact the environment [39,40]. Microbes metabolize a wide range of compounds, which affects the dynamics of organic matter and CO_2 emissions [41–43], potentially impacting agricultural productivity, ocean nutrient balance, and the global climate [43]. For example, heterotrophic microbes respire 60 gigatonnes of terrestrial organic matter annually, roughly six times the annual anthropogenic emissions. Given that microbes utilize multiple nutrients in most growth environments, understanding the interplay between different nutrients, as explored in this study, could pave the way for more informed research in ecological systems, and even aid in mitigating the environmental impact of agriculture and the biotechnology industry by decreasing CO_2 emissions.

Nutrient utilization efficiency is important in other contexts, including evolution, microbiome-host interactions and synthetic biology. For example, different nutrient combinations have been shown to impact the gut microbiome [44,45], sometimes unintuitively where supplementation of another nutrient such as an amino acid reduces the overall biomass gain of gut bacteria [46]. Our observation showing the effects of amino acid supplementation on the overall biomass yield and specifically the reduced biomass gain due to supplementation of methionine could help elucidate the phenomenon. The analysis presented here was done for a single organism and experimentally tested on *E. coli*, but since the abstracted reactions occur in any metabolic system our approach can be extended to analyze growth of consortia or even larger ecological systems. It remains an open question whether there are general principles governing the here described mutual effects or whether each nutrient combination has its own unique mechanism in a given organism.

Materials and methods

Strains and growth essays:

In the growth essays the NCM3722 strain [47,48] as used and in the acetate secretion essay NQ1243 [19]. Each experiment was carried out in three steps: seed culture, pre-culture and experimental culture. For seed culture, one colony from fresh LB agar plate was inoculated into test tube with M9 minimal medium with 4 gr/l glucose and cultured in 37ºC shaking at 350 rpm for 8-9 hours. The cell culture was then diluted to OD_{600}=0.1-0.2 in pre-warmed shake flask with m9 minimal medium with the same base nutrient as the experiment and left to grow for two hours in 37ºC shaking at 350 rpm (pre-culture). The cell culture was then diluted to OD_{600}=0.03-0.08 in pre-warmed 96 deep well plate with 1 ml. Each well contained medium with the experimental growth conditions (M9 minimal medium with nutrients according to experiment, each condition was set in triplicates) and mixed thoroughly. 200 µl cell culture from every well was then transferred to 96 deep well transparent essay plate and placed in Tecan microplate reader (Tecan infinite M200) for growth measurement. Microplate reader was programmed to maintain temperature at 37ºC, maximal shaking and measure OD_{600} every 10 minutes.

Data analysis:

The OD measured by the microplate reader was linearized using a premeasured calibration curve. Growth curves obtained in the microplate reader were compared to growth curves obtained in shake flask and were equivalent. The optical density was then converted to dry weight according to known calibration $0.396\frac{gDW}{L\ OD}$ [49]. The final biomass point was recorded at 3-5 hours after maximal OD was reached. All linear fits were done to the average of the triplicate measurements by method of least-mean-square [50] in the range that displayed a clear linear trend.

Acetate secretion rate experiment:

The experiment was done at 37ºC shaker shaking at 350 rpm in three steps: seed culture, pre-culture and experimental culture. For seed culture, one colony from fresh LB agar plate was inoculated into test tube with M9 minimal medium with 4 gr/l glucose and cultured in 37ºC

shaking at 350 rpm for 8-9 hours. The culture was then diluted in pre-warmed 96 deep well plate to an OD_{600} of 0.05-0.4 so that all cultures reached exponential phase at the same time. Each growth condition in the deep well plate was run in triplicates. All conditions contained m9 minimal medium, 4 gr/l glucose and different concentrations of the inducer for the glucose uptake promoter 3methyl-benzyl. Half of the growth conditions contained 0.1 gr/l methionine. Every 30 min, 40 µl culture from every well were collected and used to measure OD_{600} using Tecan microplate reader (Tecan Infinite M200). Another 100 µl culture from every well was collected, centrifuged at 15,000 rpm, the supernatant was collected and immediately frozen.

Supernatant were used to measure acetate concentrations using Acetate assay kit (Megazyme Acetic Acid Assay Kit). The slope of the plot of acetate concentrations versus OD_{600} for all replicates (multiplied with the measured growth rate) was used to determine the acetate secretion rate.

Supplementary material

All supplementary material is available at: https://doi.org/10.5281/zenodo.8359121.

Acknowledgments

OGo and US acknowledge support by Marie Skłodowska-Curie Actions ITN “SynCrop” (grant agreement no. 764591). Figures were generated using Biorender.

Figures

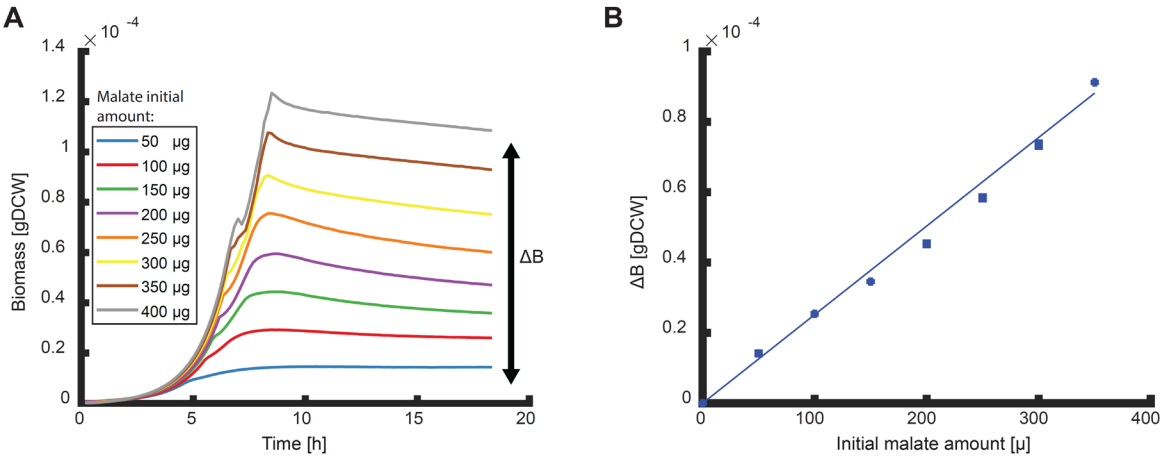

Figure 1. Overall biomass yield of malate. (A) Growth curves of *E. coli* for different initial amounts of malate. Curves are averages of three biological replicates. The produced biomass (ΔBM) is the final biomass reached in stationary phase minus the initial biomass at inoculation. **(B)** The produced biomass of the different growth curves in Fig 1A as function of the initial nutrient amount. The slope of the linear fit is the overall biomass yield (fit parameter R^2>0.9). Bars of standard errors of the biological replicates are too small to be noticeable. Data for glucose and aspartate experiments are shown in S1 Fig.

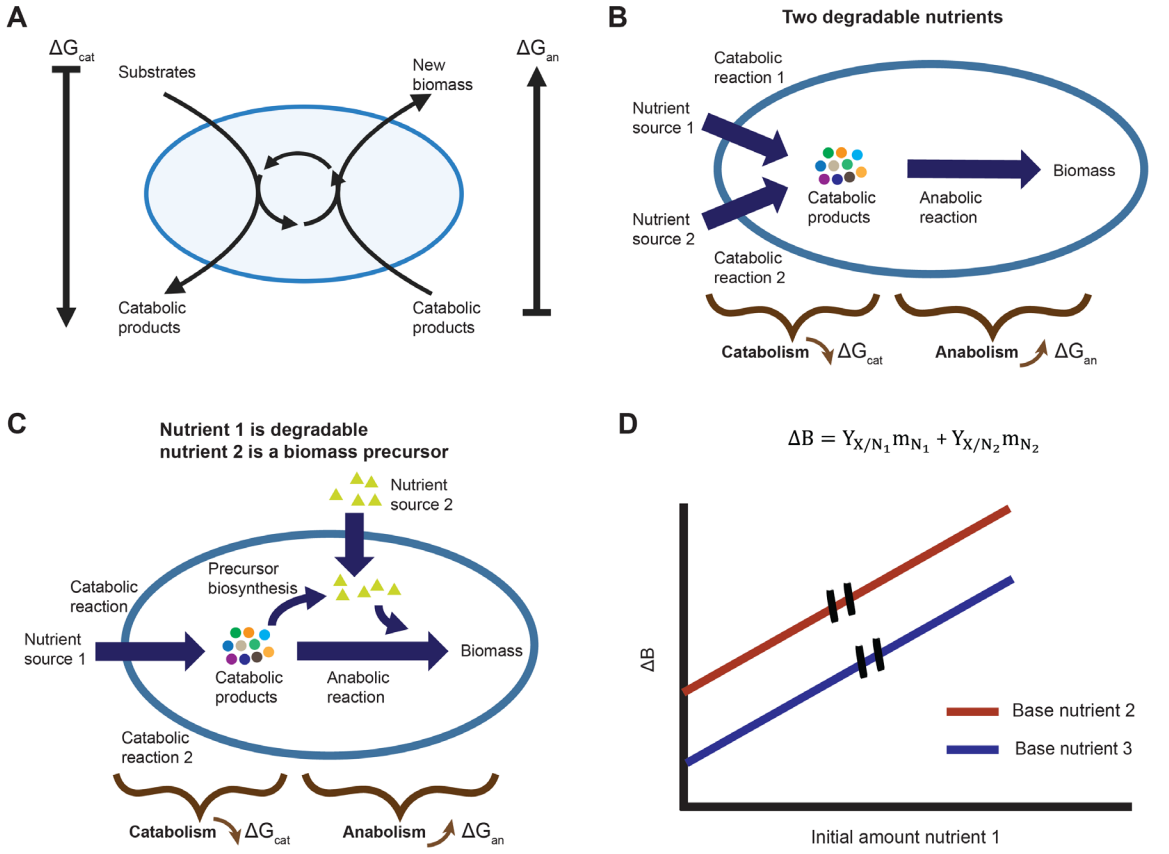

Figure 2 Expansion of black box model to include multiple nutrients. (A) The overall growth process is split into two reactions – a catabolic process in which free energy is released and an anabolic process in which new biomass is formed. The ring in the middle of the cell represents the coupling of anabolism and catabolism by ATP and other biochemical process. **(B)** Schematics of black box model expansion for two degradable nutrients. A catabolic reaction is added for each nutrient. **(C)** Schematics of model expansion for a combination of a degradable nutrient and a second nutrient that can only be used as a biomass precursor. The anabolic reaction is separated into two reactions – one for the biosynthesis of the biomass precursor and a second for the rest of the anabolic process excluding the biosynthesis reaction of the biomass precursor. **(D)** Black box model prediction for growth on two nutrient sources without mutual effect. The model predicts the produced biomass is a linear sum of the biomass gained from each nutrient. The overall biomass yield, the slope of the curve, is independent of availability of different nutrients.

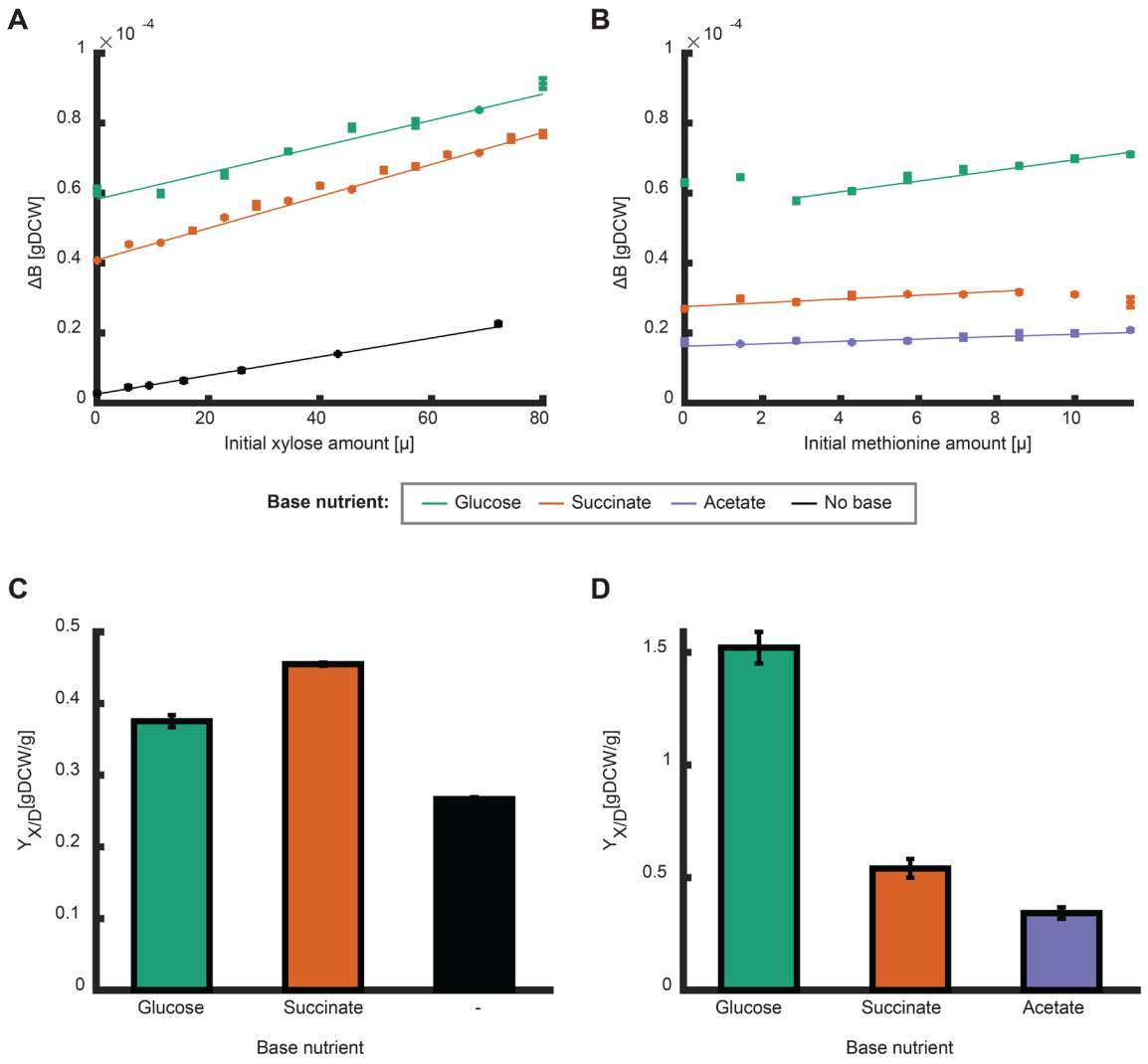

Figure 3. Produced biomass and biomass yield on different nutrient bases. (A-B) The produced biomass as function of initial amounts of the measured nutrients: xylose with or without different base nutrient sources (A, black– no base, green – 160 μg glucose, orange – 160 μg succinate), and methionine with different base nutrient sources (B, green – 160 μg glucose, orange – 80 μg succinate, purple – 160 μg acetate). Error bars depicting standard error for three biological replicates are in several cases not visible. Curves show a linear fit to the average of the three biological replicates of the linear region (fit parameter R^2>0.9). **(C-D)** The overall biomass yield (slope of the fits above) for xylose and methionine for growth on the different base nutrients. Black bar depicts growth with no base nutrient. Error bars depict error of fit parameter. The overall biomass yield is dependent on the nutrient base.

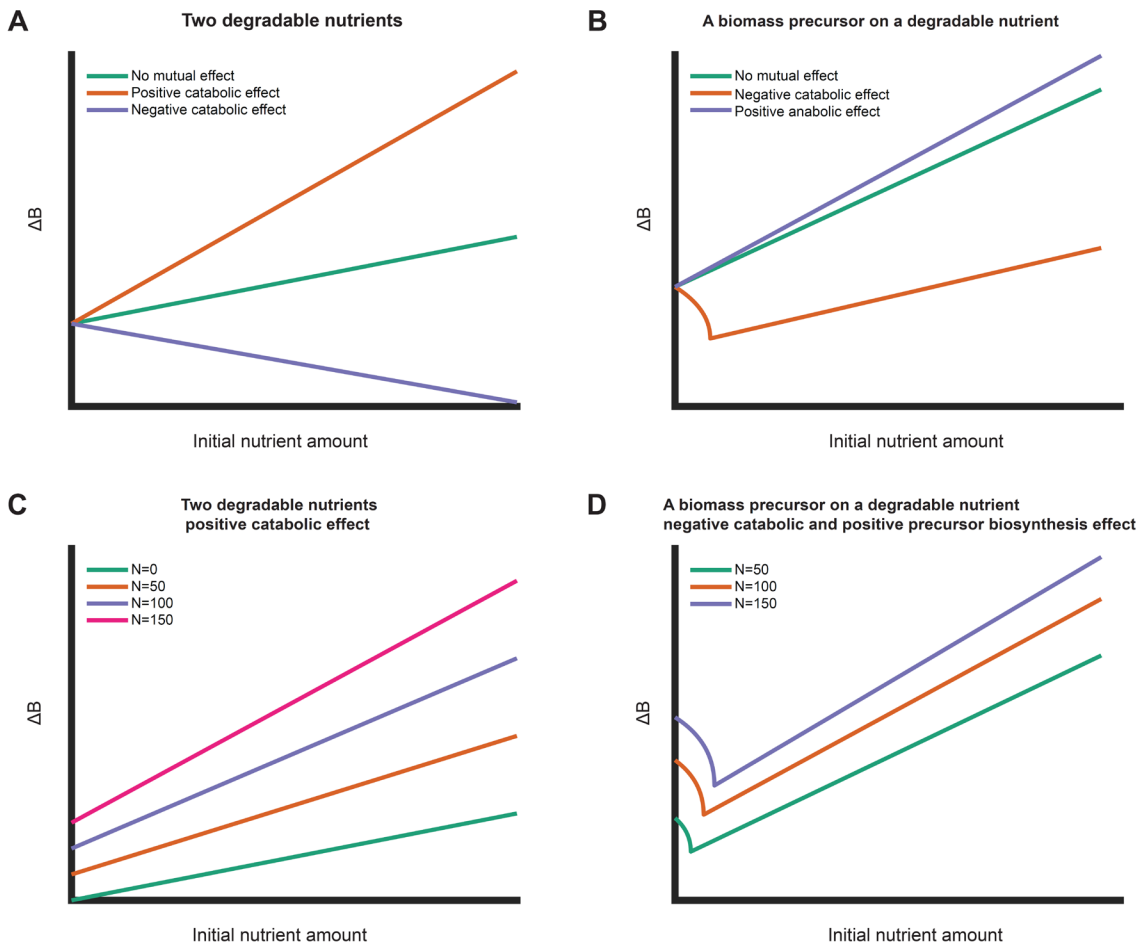

Figure 4. Expanded model prediction including mutual effects between two nutrients. **(A-B)** Simulations of expanded model with different mutual effects for growth on two degradable nutrient sources (A) and a biomass precursor in combination with a degradable nutrient (B). Initial nutrient amount of the base nutrient were kept constant in all simulations. **(C)** Simulations of expanded model for growth on two degradable nutrients for different initial amounts of base nutrient with positive catabolic mutual effect. The overall biomass yield (slope) increases with increasing initial amount of base nutrient. **(D)** Simulations of expanded model for growth on a biomass precursor and a degradable base nutrient with a negative catabolic effect and positive effect on precursor biosynthesis. Increased initial amount of base nutrient shifts the initial decreasing part and increases the slope (the overall biomass yield) of the linear part.

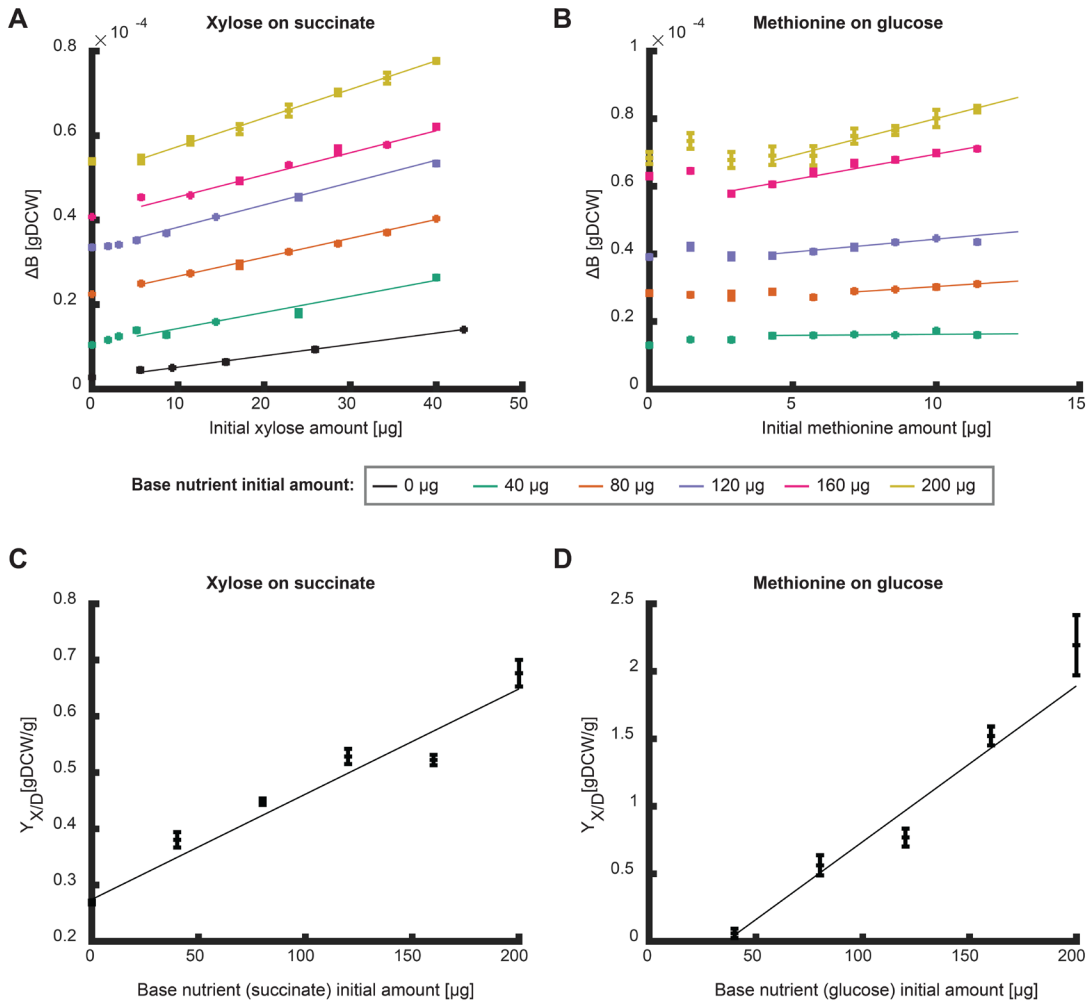

Figure 5. Effects of initial amounts of base nutrients on the overall biomass yield. (A-B) The produced biomass as a function of the initial amount of xylose (A) and methionine (B) at different initial amounts of the base nutrient succinate (A) and glucose (B)**.** Data points are average of three biological replicates and error bars are standard error that are too small to notice. Curves are linear fits in the linear region to the average of the three biological replicates (fit parameter R^2>0.9 for all fits except for methionine on 40 µg glucose which showed a good fit to a constant (p-value<0.05)). **(C-D)** The overall biomass yield as a function of initial nutrient amount as calculate from the conditions in A-B. Curves show linear fit region (fit parameter R^2>0.9). Error bars depict error of fit parameter.

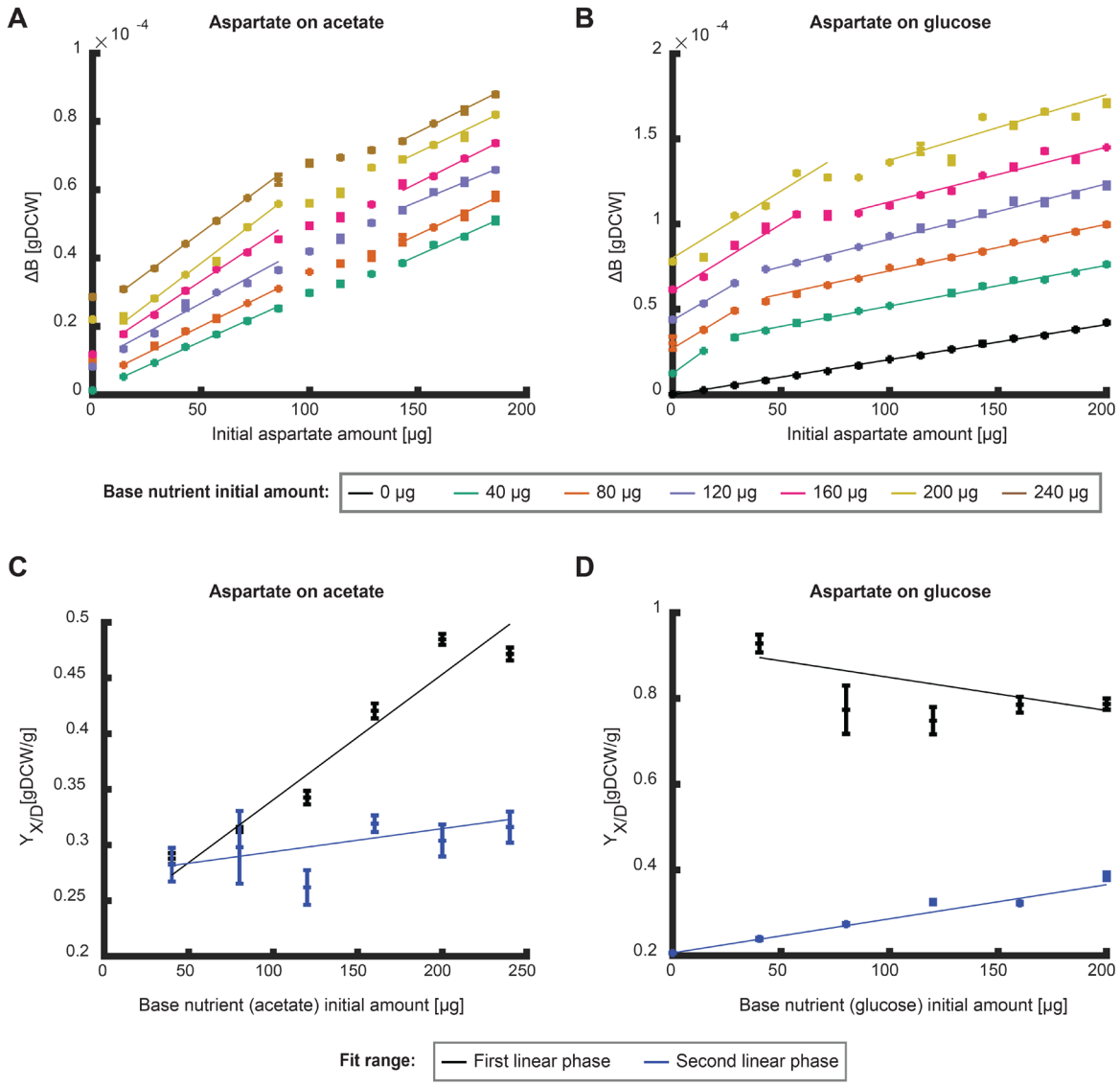

Figure 6. Effects of initial amounts of base nutrients on the overall biomass yield. (A-B) The produced biomass as function of initial nutrient amount of aspartate for different initial amounts of the base nutrient ((A) – glucose, (B) – acetate)**.** Data points are average of three biological replicates and error bars are standard error that are too small to notice. Curves are linear fits to the average of the three replicates in the linear regions (fit parameter R^2>0.9). **(C-D)** The overall biomass yield as function of initial nutrient amount as calculated from the conditions in A-B respectively. Black data points show the slope of the first linear phase and blue data points show the second. Curves show linear fit (fit parameter R^2>0.9 for first linear fit on acetate and second linear phase on glucose, the other fits show a good fit to a constant (p-value<0.05)). Error bars depict error of fit parameter.

References

1. Stocker R. Marine microbes see a sea of gradients. Science. 2012. pp. 628–633. doi:10.1126/science.1208929

2. Odum WE, Odum EP, Odum HT. Nature's pulsing paradigm. Estuaries. 1995;18: 547–555. doi:10.2307/1352375

3. Roller BRK, Schmidt TM. The physiology and ecological implications of efficient growth. ISME Journal. 2015;9: 1481–1487. doi:10.1038/ismej.2014.235

4. Koch AL. Oligotrophs versus copiotrophs. Bioessays. 2001;23: 657–661.

5. Malik AA, Martiny JBH, Brodie EL, Martiny AC, Treseder KK, Allison SD. Defining trait-based microbial strategies with consequences for soil carbon cycling under climate change. ISME J. 2020;14: 1–9.

6. Ho A, Di Lonardo DP, Bodelier PLE. Revisiting life strategy concepts in environmental microbial ecology. FEMS Microbiol Ecol. 2017;93.

7. Pirt SJ. Principles of microbe and cell cultivation. Blackwell Scientific Publications.; 1975.

8. Russell JB, Cook GM. Energetics of bacterial growth: balance of anabolic and catabolic reactions. Microbiol Rev. 1995;59: 48–62.

9. Novick A, Szilard L. Description of the chemostat. Science. 1950;112: 715–716.

10. Von Stockar U, Maskow T, Liu J, Marison IW, Patiño R. Thermodynamics of microbial growth and metabolism: An analysis of the current situation. J Biotechnol. 2006;121: 517–533. doi:10.1016/j.jbiotec.2005.08.012

11. Heijnen JJ. In search of a thermodynamic description of biomass yields for chemotrophic growth of microorganisms. Pure and Applied Chemistry. 1993;65: 1887–1888. doi:10.1351/pac199365091887

12. Liu JS, Vojinović V, Patiño R, Maskow T, von Stockar U. A comparison of various Gibbs energy dissipation correlations for predicting microbial growth yields. Thermochim Acta. 2007;458: 38–46. doi:10.1016/j.tca.2007.01.016

13. Hibbing ME, Fuqua C, Parsek MR, Peterson SB. Bacterial competition: surviving and thriving in the microbial jungle. Nat Rev Microbiol. 2010;8: 15–25. doi:10.1038/nrmicro2259

14. Rohmer L, Hocquet D, Miller SI. Are pathogenic bacteria just looking for food? Metabolism and microbial pathogenesis. Trends Microbiol. 2011;19: 341–348. doi:https://doi.org/10.1016/j.tim.2011.04.003

15. Cross WF, Benstead JP, Frost PC, Thomas SA. Ecological stoichiometry in freshwater benthic systems: recent progress and perspectives. Freshw Biol. 2005;50: 1895–1912.

16. Monod J. a Certain Number. Annual Reviews in M. 1949;3: 371–394.

17. van Niel CB. the Culture, General Physiology, Morphology, and Classification of the Non-Sulfur Purple and Brown Bacteria. Bacteriol Rev. 1944;8: 1–118. doi:10.1128/mmbr.8.1.1-118.1944

18. Myers JA, Curtis BS, Curtis WR. Improving accuracy of cell and chromophore concentration measurements using optical density. BMC Biophys. 2013;6: 1–16.

19. Basan M, Hui S, Okano H, Zhang Z, Shen Y, Williamson JR, et al. Overflow metabolism in Escherichia coli results from efficient proteome allocation. Nature. 2015;528: 99–104. doi:10.1038/nature15765

20. Leisinger T. Escherichia coli and Salmonella typhimurium: cellular and molecular biology. American Society for Microbiology. 1987; 345–351.

21. Erickson DW, Schink SJ, Patsalo V, Williamson JR, Gerland U, Hwa T. A global resource allocation strategy governs growth transition kinetics of Escherichia coli. Nature. 2017;551: 119–123. doi:10.1038/nature24299

22. Siegal ML. Shifting sugars and shifting paradigms. PLoS Biol. 2015;13: e1002068.

23. Monod J. Recherches sur la croissance des cultures bacteriennes. 1942.

24. Gommers PJF, Van Schie BJ, Van Dijken JP, Kuenen JG. Biochemical limits to microbial growth yields: an analysis of mixed substrate utilization. Biotechnol Bioeng. 1988;32: 86–94.

25. Wang X, Xia K, Yang X, Tang C. Growth strategy of microbes on mixed carbon sources. Nat Commun. 2019;10: 1279. doi:10.1038/s41467-019-09261-3

26. Lendenmann U, Egli T. Kinetic models for the growth of Escherichia coli with mixtures of sugars under carbon-limited conditions. Biotechnol Bioeng. 1998;59: 99–107.

27. Zinn M, Witholt B, Egli T. Dual nutrient limited growth: models, experimental observations, and applications. J Biotechnol. 2004;113: 263–279.

28. Payne WJ, Williams ML. Carbon assimilation from simple and complex media by prototrophic heterotrophic bacteria. Biotechnol Bioeng. 1976;18: 1653–1655.

29. Fonte ES, Amado AM, Meirelles-Pereira F, Esteves FA, Rosado AS, Farjalla VF. The combination of different carbon sources enhances bacterial growth efficiency in aquatic ecosystems. Microb Ecol. 2013;66: 871–878.

30. Del Giorgio PA, Cole JJ. Bacterial growth efficiency in natural aquatic systems. Annu Rev Ecol Syst. 1998; 503–541.

31. Daneri G, Riemann B, Williams PJ leB. In situ bacterial production and growth yield measured by thymidine, leucine and fractionated dark oxygen uptake. J Plankton Res. 1994;16: 105–113.

32. Lee C. Dissolved free amino acids, combined amino acids, and DNA as sources of carbon and nitrogen to marine bacteria. Mar Ecol Prog Ser. 1993;98: 135–148.

33. Kirchman DL. Limitation of bacterial growth by dissolved organic matter in the subarctic Pacific. Marine ecology progress series Oldendorf. 1990;62: 47–54.

34. Gommers PJF, Van Schie BJ, Van Dijken JP, Kuenen JG. Biochemical limits to microbial growth yields: an analysis of mixed substrate utilization. Biotechnol Bioeng. 1988;32: 86–94.

35. Bruinenberg PM, Jonker R, van Dijken JP, Scheffers WA. Utilization of formate as an additional energy source by glucose-limited chemostat cultures ofCandida utilis CBS 621 andSaccharomyces cerevisiae CBS 8066. Arch Microbiol. 1985;142: 302–306.

36. Van Verseveld HW, Boon JP, Stouthamer AH. Growth yields and the efficiency of oxidative phosphorylation of Paracoccus denitrificans during two-(carbon) substrate-limited growth. Arch Microbiol. 1979;121: 213–223.

37. Wilken SE, Frazão VV, Saadat NP, Ebenhöh O. The view of microbes as energy converters illustrates the trade-off between growth rate and yield. Biochem Soc Trans. 2021;49: 1663–1674.

38. Saadat NP, Nies T, Rousset Y, Ebenhöh O. Thermodynamic Limits and Optimality of Microbial Growth. Entropy. 2020. doi:10.3390/e22030277

39. Soon W, Baliunas SL, Robinson AB, Robinson ZW. Environmental Effects of Increased Atmospheric Carbon Dioxide. Energy & Environment. 1999;10: 439–468. doi:10.1260/0958305991499694

40. Solomon S, Plattner G-K, Knutti R, Friedlingstein P. Irreversible climate change due to carbon dioxide emissions. Proceedings of the National Academy of Sciences. 2009;106: 1704–1709. doi:10.1073/pnas.0812721106

41. Karhu K, Auffret MD, Dungait JAJ, Hopkins DW, Prosser JI, Singh BK, et al. Temperature sensitivity of soil respiration rates enhanced by microbial community response. Nature. 2014;513: 81–84.

42. Frey SD, Lee J, Melillo JM, Six J. The temperature response of soil microbial efficiency and its feedback to climate. Nat Clim Chang. 2013;3: 395–398.

43. Manzoni S, Taylor P, Richter A, Porporato A, Ågren GI. Environmental and stoichiometric controls on microbial carbon-use efficiency in soils. New Phytologist. 2012;196: 79–91.

44. Wu L, Tang Z, Chen H, Ren Z, Ding Q, Liang K, et al. Mutual interaction between gut microbiota and protein/amino acid metabolism for host mucosal immunity and health. Animal Nutrition. 2021;7: 11–16.

45. Beaumont M, Roura E, Lambert W, Turni C, Michiels J, Chalvon-Demersay T. Selective nourishing of gut microbiota with amino acids: A novel prebiotic approach? Front Nutr. 2022;9: 1066898.

46. Tramontano M, Andrejev S, Pruteanu M, Klünemann M, Kuhn M, Galardini M, et al. Nutritional preferences of human gut bacteria reveal their metabolic idiosyncrasies. Nat Microbiol. 2018;3: 514–522. doi:10.1038/s41564-018-0123-9

47. Lyons E, Freeling M, Kustu S, Inwood W. Using genomic sequencing for classical genetics in E. coli K12. PLoS One. 2011;6. doi:10.1371/journal.pone.0016717

48. Soupene E, Van Heeswijk WC, Plumbridge J, Stewart V, Bertenthal D, Lee H, et al. Physiological studies of Escherichia coli strain MG1655: Growth defects and apparent cross-regulation of gene expression. J Bacteriol. 2003;185: 5611–5626. doi:10.1128/JB.185.18.5611-5626.2003

49. Myers JA, Curtis BS, Curtis WR. Improving accuracy of cell and chromophore concentration measurements using optical density. BMC Biophys. 2013;6: 1–16.

50. Bevington PR, Robinson DK, Blair JM, Mallinckrodt AJ, McKay S. Data reduction and error analysis for the physical sciences. Computers in Physics. 1993;7: 415–416.

Chapter 4 – Conclusions and outlook

Ohad Golan[1, 2]

[1] Institute of Molecular Systems Biology, ETH Zürich, Otto-Stern-Weg 3, 8093 Zürich, Switzerland

[2] Life Science Zurich PhD Program on Systems Biology, Zurich, Switzerland

Understanding the intricate nature of biological systems is an endeavor that has baffled and intrigued scientists for centuries. Biological processes are highly complex, governed by a myriad of interconnected components that work together in finely tuned networks. From the most detailed genetic mechanisms to the macro-level interactions of ecosystems, the complexity increases exponentially, encompassing a multitude of variables, feedback loops, and non-linear dynamics. This complexity often makes it difficult to predict system behavior, and even harder to manipulate systems in desired ways. Mathematical modeling, therefore, plays a crucial role in biological research. It provides a systematic framework for synthesizing known information, for revealing gaps in our understanding, and for predicting system behavior under various conditions.

While the value of mathematical modeling in biology is immense, it comes with inherent challenges and obstacles [1,2]. A significant challenge lies in the process of model formulation itself. Each model requires careful consideration of the level of detail it entails, the relevant parameters, and the most appropriate mathematical approach. Model oversimplification could potentially lead to inaccurate or incomplete predictions, while overcomplicated models may become intractable or difficult to interpret. Parameter estimation constitutes another significant challenge. Biological systems are notorious for their variability, and data for parameterization can often be noisy, incomplete, or even contradictory [3–5]. Given this inherent uncertainty in biological data, it can be challenging to quantitatively validate models to a high degree of confidence.

Given these challenges, two primary approaches have been adopted: the bottom-up and the top-down approach. The bottom-up, or fine-grained approach [1,6,7], models the system by considering all known biochemical interactions and processes within a cell. By compiling these reactions together to a single model and simulating cell behavior under varying growth conditions or genetic manipulations, this approach facilitates drawing conclusions and predictions. Conversely, the top-down, or coarse-grained approach [8,9], rather than focusing on the details of individual biochemical interactions, seeks to capture the system's overall

behavior by concentrating on higher-level properties and dynamics. This approach generally requires fewer details and may be more suitable for larger-scale, system-level analysis, where the fine-grained details are less critical to understanding the overall system behavior.

These two modeling approaches - bottom-up and top-down - are not strictly defined but rather lie on a continuum of granularity. The choice between them largely depends on the specific research questions being asked and the available data. A coarse-grained model, for example, can be expanded or refined to include more details, thereby becoming more finely grained. This flexibility allows a model to evolve and adapt as new information becomes available or as the research focus shifts. Ultimately, the level of detail incorporated into a model must balance the need for accuracy and comprehensibility with the practicalities of data availability and computational feasibility.

The work presented in this thesis set out to tackle fundamental questions in the physiology of autocatalytic systems using the top-down modeling approach. Focusing on the intricate processes of nutrient utilization in *E. coli*, our investigation sought to understand the basic laws governing nutrient utilization in both steady-state balanced growth and batch culture conditions. We honed in on the specific impact of growth on multiple nutrient sources – the reality of nearly all natural and engineered biological systems. To enhance our understanding and generate robust conclusions, we expanded previous coarse-grained models to accommodate this multi-nutrient growth paradigm. By augmenting these models, we were able to effectively interpret our data, revealing crucial insights into the dynamics of autocatalytic systems and laying the groundwork for future research and potential applications.

Main conclusions

In **Chapter 1**, we built upon a refined coarse-grained proteome allocation model [10], extending it to encompass growth on multiple nutrient sources. This expansion facilitated a deeper understanding of the cellular processes that govern nutrient utilization and associated growth coefficients in microbial cells. Focusing on maintenance and yield coefficients during balanced growth, our model elucidated the impact of different metabolic processes – notably

the energy generating pathways of respiration and partial respiro-fermentation – on these parameters. A significant insight from our study is the impact of non-active proteome sectors on the maintenance coefficient, a measure traditionally associated exclusively with energy expenditures for maintenance processes and the efficiencies of active energy-generating pathways [11–14]. Moreover, the expanded model accurately predicted the effects of amino acid supplementation on the physiological growth coefficients. Contrasting with prior studies that calculated the cost of precursor biosynthesis based on either energetic or proteomic costs [15–19], our model offers a comprehensive assessment, incorporating both these aspects to quantify the total cost of precursor biosynthesis.

Chapter 2 offers a comprehensive study exploring how nutrient availability impacts an organism's nutrient utilization efficiency, with a particular emphasis on biomass generation in a closed environment such that all available nutrients are fully utilized. Our research expands on existing black box models [20,21], innovatively extending them to accommodate growth based on multiple nutrient sources with differing utilization characteristics. This includes degradable nutrients that require degradation prior to utilization, such as sugars, non-degradable biomass precursors like certain amino acids that can only be directly used for biomass biosynthesis, and degradable biomass precursors like some amino acids that can be used both directly for biomass biosynthesis and degraded for energy and carbon.

The developed model qualitatively reflects experimental observations and predicts that the overall biomass gain is influenced not only by the availability of different nutrients but also by their initial proportions. This conclusion challenges the traditional perspective that the yield of a chemotrophic organism is exclusively dependent on the nutrients' reduction level [20–22]. Furthermore, we found that supplementing a specific nutrient can potentially lead to a decrease in the utilization efficiency of another - a phenomenon exemplified by *E. coli's* growth pattern in the presence of methionine and glucose. Although our model's coarse granularity precludes detailing specific metabolic pathways, it facilitates the identification of which growth processes

- catabolism, anabolism, or biomass precursor synthesis - are influenced by each nutrient combination, thereby encouraging the generation of novel hypotheses.

Beyond its immediate insights, our approach paves the way for further investigation of larger ecological systems and microbial consortia, stimulating intriguing questions for future research. For example, are there universal principles governing nutrient interactions, or does each nutrient pairing cultivate its unique mechanisms within specific organisms? These questions invite further exploration.

Outlook

Integrating insights from both models

A common thread uniting both chapters of this thesis is the investigation of biomass yield. In Chapter 1, we explore yield in the context of steady-state balanced growth, Chapter 2 focuses on the comprehensive biomass yield in batch culture conditions where all available nutrients are fully consumed, including the reutilization of secreted byproducts. Each chapter expands a previous model grounded in differing basic assumptions, tailoring them to align with the respective experimental growth conditions. In Chapter 1, the model hinges on the assumption of balanced growth, whereas Chapter 2 builds on the black box model, which stipulates that the yield is solely predicated on the dissipation energy of the available nutrients.

The natural progression of our research suggests a comparison of these models as the next logical step. Such a comparative analysis could shed light on the mechanistic cause behind the mutual effect between nutrients as observed in Chapter 3, as well as reveal other factors that differentiate the overall yield in batch cultures from the yield observed in steady-state conditions. To facilitate this, the steady-state model needs to be extrapolated across the full growth curve. Essentially, the model would need to be solved for every growth condition that the cells experience throughout the curve: beginning with the availability of all nutrients, proceeding to post-depletion of a particular nutrient, and continuing to growth on secreted byproducts, both with and without each nutrient. The sum of the solutions of the full curve would then be compared to the solution of the expanded black box model.

Metabolic Models: Current Landscape, Contributions, and Future Directions

In the current landscape of metabolic research, an array of distinct metabolic models exists, each characterized by its unique mathematical formulation and the algorithm employed for solving the system. The work presented in this thesis extends this body of knowledge by introducing and refining two such models based on pre-existing ones: a coarse-grained proteome allocation model (Chapter 1), and a black box model (Chapter 2).

One of the fundamental assumptions underpinning the proteome allocation model in Chapter 1 is the law of conservation of mass, a foundational principle in physics that also encompasses the balance of energy. The black box model in Chapter 2, on the other hand, rests on the laws of thermodynamics, where the required energy for biomass biosynthesis is derived from nutrient degradation. At their core, these assumptions are equivalent and provide a solid foundation for understanding metabolic processes.

The key distinction between the two models, however, lies not in their mathematical representation, but in the set of underlying assumptions each one adopts. For instance, assumptions regarding proteome allocation and the mass balance of carbon form a part of the model in Chapter 1 but are absent in Chapter 2. Thus, what differentiates one model from another is essentially the selection and prioritization of assumptions rather than the formulation of the mathematical representation itself.

Similarly, other metabolic models in use today can be differentiated more by the assumptions they accommodate than by their mathematical constructs. Consequently, one of the future directions in metabolic modeling is to devise a flexible mathematical representation that can account for or disregard a broad spectrum of possible constraints and assumptions as needed, as well as capture all levels of granularity.

To elucidate this concept, let's draw an analogy to the mathematical representation of waves. Historically, sound waves, sea waves, waves on a string, and electromagnetic waves were all described as distinct phenomena. However, a comprehensive mathematical description revealed that they all behave according to the same principles as described by the wave

equation. The distinctions among these various wave phenomena lie in their dimensionality and specific parameters. Thus, what initially appeared to be disparate phenomena are, in fact, fundamentally similar. The insights gained from studying one system can be extrapolated and applied to the others.

In a parallel manner, different autocatalytic systems are often studied separately, even though, at their core, they adhere to the same set of constraints outlined in the introduction, albeit with varying parameters and levels of granularity. The development of a unified, overarching description of the autocatalytic system could potentially enable the transfer of conclusions and understandings between systems, akin to the cross-applications observed in wave studies.

Such a unified model would foster clearer discussions and enhance communication in the field, thereby helping researchers to understand and communicate the core principles and assumptions underpinning their models more effectively. Moreover, a flexible, assumption-based model would hold great potential for application beyond biological systems. For example, it could be adapted for use in non-biological living systems such as economic systems, as alluded to in the introduction.

Potential real-world applications

The work presented in this thesis is driven by a commitment to answer fundamental questions in science. While the quest for understanding for its own sake is a worthy pursuit, we also acknowledge the potential applications that could arise from these explorations.

One particularly promising direction lies within the realm of healthcare. Today, one of the most formidable challenges healthcare faces is the growing resistance to antibiotics of bacterial infections. Increasingly, infections are developing resistance to these critical drugs, leading to a significant rise in mortality rates [23].

An intersection of our research lies with this healthcare challenge. The models developed in this thesis could potentially be expanded to support antibiotic treatments with appropriate nutritional supplementation. By understanding the nutrient utilization of bacteria and their

growth under various nutrient combinations, we could potentially devise nutrition plans that limit the growth of infections and simultaneously augment the effect of antibiotics. For example, we observed that supplementation of certain nutrients such as the amino acid methionine decreased the biomass gain of *E. coli* in batch culture. Supplementing the correct nutrient could potentially also decrease the biomass gain of infectious agents and limit their growth. This approach holds promise in contributing significantly to the ongoing battle against antibiotic resistance, thereby demonstrating the real-world impact of our research.

After healthcare, another sector that stands to benefit from our research is environmental science, particularly in the area of global climate. Carbon sequestration serves as a critical tool for mitigating the impacts of climate change by capturing and storing atmospheric CO_2—a key greenhouse gas. Building on this concept, our work on efficient nutrient utilization could be particularly useful for enhancing carbon capture technologies that rely on bacteria or extended to photosynthetic organisms like algae. By leveraging the insights gained from our metabolic models to better understand nutrient interactions, we could potentially improve the efficiency of existing carbon sequestration methods. This broadens the scope of our research's applicability, extending its reach beyond the primary focus of metabolic processes.

References

1. Gu C, Kim GB, Kim WJ, Kim HU, Lee SY. Current status and applications of genome-scale metabolic models. Genome Biol. 2019;20: 1–18.

2. Vasilakou E, Machado D, Theorell A, Rocha I, Nöh K, Oldiges M, et al. Current state and challenges for dynamic metabolic modeling. Curr Opin Microbiol. 2016;33: 97–104. doi:https://doi.org/10.1016/j.mib.2016.07.008

3. Pilpel Y. Noise in biological systems: pros, cons, and mechanisms of control. Yeast Systems Biology: Methods and Protocols. 2011; 407–425.

4. Tsimring LS. Noise in biology. Reports on Progress in Physics. 2014;77: 026601.

5. Eling N, Morgan MD, Marioni JC. Challenges in measuring and understanding biological noise. Nat Rev Genet. 2019;20: 536–548.

6. O'Brien EJ, Monk JM, Palsson BO. Using Genome-scale Models to Predict Biological Capabilities. Cell. 2015;161: 971–987. doi:https://doi.org/10.1016/j.cell.2015.05.019

7. Price ND, Reed JL, Palsson BØ. Genome-scale models of microbial cells: evaluating the consequences of constraints. Nat Rev Microbiol. 2004;2: 886–897.

8. Doan DT, Hoang MD, Heins A-L, Kremling A. Applications of Coarse-Grained Models in Metabolic Engineering. Front Mol Biosci. 2022;9.

9. Chen Y, Nielsen J. Mathematical modeling of proteome constraints within metabolism. Curr Opin Syst Biol. 2021;25: 50–56.

10. Basan M, Hui S, Okano H, Zhang Z, Shen Y, Williamson JR, et al. Overflow metabolism in Escherichia coli results from efficient proteome allocation. Nature. 2015;528: 99–104. doi:10.1038/nature15765

11. Pirt SJ. The maintenance energy of bacteria in growing cultures. Proc R Soc Lond B Biol Sci. 1965;163: 224–231.

12. Van Bodegom P. Microbial maintenance: a critical review on its quantification. Microb Ecol. 2007;53: 513–523.

13. Marr AG, Nilson EH, Clark DJ. The maintenance requirement of Escherichia coli. Ann N Y Acad Sci. 1963;102: 536–548.

14. Zamboni N, Mouncey N, Hohmann H-P, Sauer U. Reducing maintenance metabolism by metabolic engineering of respiration improves riboflavin production by Bacillus subtilis. Metab Eng. 2003;5: 49–55.

15. Kaleta C, Schäuble S, Rinas U, Schuster S. Metabolic costs of amino acid and protein production in Escherichia coli. Biotechnol J. 2013;8: 1105–1114. doi:10.1002/biot.201200267

16. Barton MD, Delneri D, Oliver SG, Rattray M, Bergman CM. Evolutionary systems biology of amino acid biosynthetic cost in yeast. PLoS One. 2010;5: e11935.

17. Chen Y, Nielsen J. Yeast has evolved to minimize protein resource cost for synthesizing amino acids. Proceedings of the National Academy of Sciences. 2022;119: e2114622119.

18. Swire J. Selection on Synthesis Cost Affects Interprotein Amino Acid Usage in All Three Domains of Life. J Mol Evol. 2007;64: 558–571. doi:10.1007/s00239-006-0206-8

19. Heizer Jr EM, Raiford DW, Raymer ML, Doom TE, Miller R V, Krane DE. Amino acid cost and codon-usage biases in 6 prokaryotic genomes: a whole-genome analysis. Mol Biol Evol. 2006;23: 1670–1680.

20. Liu JS, Vojinović V, Patiño R, Maskow T, von Stockar U. A comparison of various Gibbs energy dissipation correlations for predicting microbial growth yields. Thermochim Acta. 2007;458: 38–46. doi:10.1016/j.tca.2007.01.016

21. Von Stockar U, Maskow T, Liu J, Marison IW, Patiño R. Thermodynamics of microbial growth and metabolism: An analysis of the current situation. J Biotechnol. 2006;121: 517–533. doi:10.1016/j.jbiotec.2005.08.012

22. Heijnen JJ. In search of a thermodynamic description of biomass yields for chemotrophic growth of microorganisms. Pure and Applied Chemistry. 1993;65: 1887–1888. doi:10.1351/pac199365091887

23. Odonkor ST, Addo KK. Bacteria resistance to antibiotics: recent trends and challenges. Int J Biol Med Res. 2011;2: 1204–1210.

Acknowledgments

The work presented in this thesis was done in the sole purpose of expanding our understanding of the natural world. It is the outcome of over ten years of dedicated study, over half of which were spent at ETH. I seize this opportunity to express my deep gratitude to all those that contributed in various ways to this endeavor.

First and foremost, I must thank my close family – **Hanan, Ronit, Nadav** and **Amir.** Your endless love, care and support during these years, and before, have been invaluable. Though I may not often verbalize my appreciation, it is not for lack of it, but rather because there are no words suitable express it.

I would like to recognize the people and institutions that have profoundly influenced this work and my scientific training prior to arriving at ETH. I am particularly grateful to my former lab members of the Sprinzak lab, **David Sprinzak,** for teaching me the fundamentals of scientific analysis and deduction, as well as the art of presenting scientific work; **Olga Loza** for showing me the tough but essential route to crafting a good presentation; and **Udi Binshtok**, **Amitai Menuchin** and **Dima Rivkin** for their unwavering support and insightful reflections. I also wish to convey my appreciation to the **Tel-Aviv University School of Physics and Astronomy**. The unparalleled education I received during my bachelor's and master's degrees at this institution have left an indelible mark on my academic journey. It is the best physics program in the world with the most caring and driven professors.

I would like to acknowledge the Sauer Group and its members. Foremost among these are my students: **Lina Eckert, Olivia Gampp, Stella Reichling** and **Priyanuj Bordoloi**. It is from you that I have learned the most, and I can only hope that you have found our time together as enriching as I have. I am grateful to **Prof. Uwe Sauer** for his guidance and support during the writing process as well as for fruitful discussions, I've learned much from him. Many thanks also go to **Pau Pérez Escriva** for his steadfast support and specifically his assistance with the experimental work despite the outcome. I am

grateful to **Christoph Gruber** for always being there for a chat, and to **Peter Doubleday** for helping to maintain my sanity.

My heartfelt thanks go out to the **Economic Principles in Cell Physiology** consortium and its branches. To **Wolfram Liebermeister** and **Elad Noor**, thank you for inviting me to participate in this extraordinary project. I would also like to express my appreciation to my co-authors of the "Coarse-grained models of growing cells" chapter, **Hidde de-Jong** and **Andrea Y. Weiße,** for the enriching collaboration and discussion. I see this chapter as one of my key contributions to science and I eagerly anticipate continuing our work. The **Young Scholars** deserve special mention for all the enlightening presentations and discussions.

Finally, I would like to extend my gratitude to all those who made my time in Zurich more comfortable. Thanks to **Hamakom** and **Chabad** for their amazing food and inviting atmosphere. To the friends from the Jewish community who provided a comforting anchor in challenging times, especially our hiking group: **Amit Moryossef**, **Noga Hoerni**, and **Magda Sikora**. Special thanks to other friends I've made along the way, notably **George** for all our shared adventures, and **Chantal Ernst** for keeping me grounded. Lastly, I want to express my gratitude to **Angelica** and **Misty Richardson** for their empowering yoga classes and teachings.

Thank you all for helping to shape this work and experience.